

## Asteroseismology of Pulsating Stars

Santosh Joshi & Yogesh C. Joshi

*Aryabhata Research Institute of Observational Sciences(ARIES), Manora Peak, Nainital 263 002, India*

Received xxx; accepted xxx

### Abstract.

The success of helioseismology is due to its capability of measuring  $p$ -mode oscillations in the Sun. This allows us to extract informations on the internal structure and rotation of the Sun from the surface to the core. Similarly, asteroseismology is the study of the internal structure of the stars as derived from stellar oscillations. In this review we highlight the progress in the observational asteroseismology, including some basic theoretical aspects. In particular, we discuss our contributions to asteroseismology through the study of chemically peculiar stars under the “Nainital-Cape Survey” project being conducted at ARIES, Nainital since 1999. This survey aims to detect new rapidly-pulsating Ap (roAp) stars in the northern hemisphere. We also discuss the contribution of ARIES towards the asteroseismic study of the compact pulsating variables. We comment on the future prospects of our project in the light of the new optical 3.6-m telescope to be install at Devasthal (ARIES). Finally, we present a preliminary optical design of the high-speed imaging photometers for this telescope.

*Key words:* Helioseismology, Asteroseismology, Pulsations, Stellar Structure, Chemically Peculiar Stars

### 1. Introduction

The conference entitled “Plasma Processes in Solar and Space Plasma at Diverse Spatio-Temporal Scales : Upcoming Challenges in the Science and Instrumentation” took place during 26-28 March 2014 when the preparation for the installation of the 3.6-m telescope at Devasthal (ARIES) is going on and the state-of-art instruments would soon be available for the study of faint astronomical objects with high-temporal resolution. Although this conference was devoted to the study of the solar interior (helioseismology) but asteroseismology was one of the chosen topic for this conference. In the following sub-sections we give a brief introduction to the subject followed by the techniques.

### 1.1 *Variable Stars*

Many stars show light variations on a time-scale shorter than their evolutionary changes and such objects are known as variable stars. Two major groups of variable stars are known: extrinsic and intrinsic variables. The light variations in extrinsic variables are due to external factors. For example, the light variations in eclipsing binary stars is caused by two stars passing in front of each other, so that light coming from one of them is periodically blocked by another one. By analysing the light curves of eclipsing binaries, one can estimate the fundamental parameters such as their masses, radius etc. On the other hand, the light variations in intrinsic variables arise in the stars themselves. For example, as the size and shape of a star changes due to pulsations. The Sun is a variable star whose magnetic activity varies on a time-scale of approximately 11 years. However, significant variation of a period around five minutes is also observed in Sun. These short period oscillations have very low-amplitude and are only detectable due to its proximity.

The variable stars have been used to estimate various basic physical stellar parameters ever since the discovery of Mira by David Fabricius (Olbers 1850). The 11-months periodic brightness of Mira shows a 10-mag difference between minimum and maximum brightness. Shapley (1914) suggested that variability among Cepheids and cluster variables are due to internal or surface pulsations in the star itself. Pigott (1785) discovered the first pulsating  $\delta$ -Cephei (Cepheid) star and the period-luminosity (P-L) relation was discovered by Henrietta Swan Leavitt (Leavitt & Pickering 1912) which is the foundation of the cosmic distance scale.

The photometric and spectroscopic observational techniques with modest-sized telescopes of diameters 1 to 4-m are well suited for the detection and study of stellar variability. The photometric precision attained with such telescopes is normally of the order of few milli-magnitudes (mmag). Here, the limiting factor is the instability in the atmosphere caused by scintillation and extinction. The radial velocity precision attained by spectroscopy could be of the order of a cm/sec. However, the atmospheric effects does not play major role in spectroscopic observations, hence pulsations are more easily detected in comparison to the photometric observations. The prospects for high-precision photometry and spectroscopy in the field of asteroseismology are thus very promising. For this reason we are developing a high-resolution spectrograph and time-series CCD photometers for the up-coming 3.6-m telescope at Devasthal (ARIES).

### 1.2 *Helioseismology*

The Sun is an outstanding example of the stellar seismology. The five-minutes oscillatory motion in the atmosphere of the Sun was detected in

the early 1960's by Leighton et al. (1962). The oscillations observed at the surface of the Sun manifest themselves in small motions similar to the seismic waves generated at the surface of Earth during earthquakes. This discovery gave birth to the helio-seismology which has proved to be an extremely successful technique in probing the physics and dynamics of the solar interior (Christensen-Dalsgaard 2002; Basu & Antia 2008; Chaplin & Basu 2008). A large number of oscillation modes ( $\sim 10^7$ ) are thought to be simultaneously excited in Sun and each mode carries information on each part of the solar interior. When averaged over the solar disk, the perturbations due to these modes average to zero, rendering them undetectable. These studies have contributed greatly to a clearer understanding of the Sun by measuring the characteristics of the  $p$ -mode oscillation spectrum.

Solar oscillations are the result of the excitation of global modes by convective motion (forced oscillations) where pressure is the restoring force ( $p$ -modes). On the surface of Sun, these oscillations are observed as Doppler shifts of spectrum lines with amplitudes of individual modes not exceeding 0.1 m/sec or as whole-disk luminosity variations with amplitudes not exceeding a few part per million (ppm). The observational confirmation of the five-minutes oscillations was done by Deubner (1975) and Rhodes et al. (1977). Ulrich (1970) and Leibacher & Stein (1971) proposed that the waves observed on the surface of Sun are standing-wave in nature. The periods of solar-oscillations are in the range of 3–15 min with peak amplitudes around 5-min (Fletcher et al. 2010). A number of studies have also been claimed the detection of  $g$ -modes in the Sun (García et al. 2008; Appourchaux et al. 2010)) but more studies are required for their confirmation. This proceedings contain many articles on helioseismology where further details can be found.

### 1.3 From Helioseismology to Asteroseismology

During the last decades, many observational and theoretical efforts in the study of the acoustic modes of solar oscillations have brought to a detailed knowledge of the interior of the Sun. The large stellar distance, the point source character of the stars, the low-amplitude of the oscillations and effect of the earth's atmosphere on the signal restrict the asteroseismic studies to the use of the small sets of data often characterized by modes with only low-harmonic degree ( $l < 3$ ). As we know the Sun oscillates in thousands of non-radial eigenmodes, and this richness in the number of identified modes leads to the great success of helioseismology using which one can probe the invisible internal structure of the Sun in detail. Using the ground based Birmingham Solar-Oscillations Network (BiSON, Chaplin et al. 1996) more than 70 independent modes with amplitude of few ppm and periods between 3–15 minutes were detected and identified as low-degree ( $l$ ) pulsation modes ( $l \leq 3$ ) that can be used to probe the solar core (Chaplin et al. 2007). De-

tection of solar-like oscillations in stars is, however, very difficult because of their small amplitudes. The study of stellar oscillations (asteroseismology) have several advantages over the other observables because frequencies, amplitude and phase of the oscillations can be measured very accurately which depends upon the equilibrium structure of the model. Different modes of pulsations are confined and probe different layers of the interiors of the stars, thus accurate measurements of acoustic frequencies can be used not only to study the stellar interiors but also constraints on the theories of stellar evolution.

The measurements of basic physical parameters such as luminosity, effective temperature, surface composition and  $v \sin i$  (from spectrum analysis) age (estimated through stars in cluster), masses and radii (measured using the spectroscopic binaries) are affected by unknown effects such as loss, accretion and diffusion of mass. Therefore, the structure of the model of the stars can not be so well constrained such as that of the Sun. As a result, the precision attained by asteroseismology is much less than that obtained by helioseismic studies. Nevertheless, several attempts have been made during recent times with the aim to identify oscillations in distance stars and also to model the stellar pulsation phenomena. In particular, photometric observations obtained from space by the *MOST*<sup>1</sup>, *CoRoT*<sup>2</sup> and *Kepler*<sup>3</sup> missions have led to in-depth understanding of asteroseismology by detection of hundreds of stars with solar-like oscillations.

## 2. Asteroseismology

Just as helioseismology has led to new insights on the internal structure of the Sun, asteroseismology provides wealth of information on the physical properties of many different types of stars. To extract this information, the observed pulsational frequencies are compared to the frequencies predicted by a stellar model. The input physical parameters of the models are adjusted to agree with observations. If a model succeeds in reproducing the observed frequencies, it is called a seismic model. The applications of asteroseismology are used: (1) for the accurate and precise estimates of the stellar properties (i.e., density, surface gravity, mass, radius and age); (2) an additional information on the internal rotation and angle of inclination can also derived for a better understanding of the dynamics of the star; (3) to estimate the angle between the stellar rotation axis, the line-of-sight, magnetic axis and pulsation axis, (4) to bring additional constraints on stellar

---

<sup>1</sup><http://www.astro.ubc.ca/MOST/>

<sup>2</sup><http://corot.oamp.fr/>

<sup>3</sup><http://www.kepler.arc.nasa.gov/>

models which allow more precise estimation of age, and (5) to derive the strength of magnetic field.

### 3. Stellar Pulsations

The pulsation of a star is characterized by expansion followed by contraction. If the pulsating star preserves its spherical symmetry then mode of pulsation is known as the radial. Otherwise the pulsation called as non-radial. Many stars, including the Sun, pulsate simultaneously in many different radial and non-radial modes. Stars such as Cepheids and RR Lyra pulsate either in one or two radial modes. The physical basis for understanding stellar pulsations has been described with great clarity and a great detail by many authors (see, for instance, Cox 1980; Unno et al. 1989; Christensen-Dalsgaard & Berthomieu 1991; Brown & Gilliland 1994; Aerts et al. 2010; Balona 2010). Here we present only the minimal description necessary for our purpose.

When a small contraction occurs, the local temperature slightly increases, inducing an enhancing the outward pressure. Hence, the layer expands again until the equilibrium is attained. The time requires to recover from such a small contraction is given by the dynamical time-scale of the star:

$$t_{\text{dyn}} = \left( \frac{R^3}{GM} \right)^{1/2} \propto (G\bar{\rho})^{-1/2} \quad (1)$$

where  $R$ ,  $G$ ,  $M$  and  $\bar{\rho}$  are the radius, Gravitational constant, mass and mean stellar density, respectively. The periods of the oscillations generally scale to  $t_{\text{dyn}}$  which is expressed as the time star needs to go back to its hydrostatic equilibrium if some dynamical process disrupts the balance between pressure and gravitational force. For a star close to hydrostatic equilibrium, this time scale is equivalent to the time it takes a sound wave to travel from the stellar center to the surface which is equivalent to the free-fall time-scale of the star). The period of oscillation of a star can not exceed the dynamical time. For the Sun,  $\tau_{\text{dyn}} \sim 20$ -min while for a white dwarf this value is less than a few tens of seconds. Thus estimation of the period immediately gives the important parameters of the star, viz. the mean density.

Fig. 1 shows a theoretical pulsational Hertzsprung-Russell (HR) diagram. Beside main-sequence (MS) pulsators (hydrogen burning in the core), there are pre-main sequence stars (nuclear reactions have not started yet) and post-main sequence stars (hydrogen burning takes place in a shell). The MS pulsating variables are excellent asteroseismic tools because most of them are multi-periodic. Along the MS one finds the early B and late O stars ( $M \sim 8$ – $20 M_{\odot}$ ) there are the  $\beta$  Cephei pulsators with periods of hours. The long-period slowly pulsating B (SPB) stars ( $M \sim 3$ – $12 M_{\odot}$ ) are mid-to late B stars with periods of days. Moving towards lower masses, there are the  $\delta$  Scuti pulsators ( $M \sim 1.5$ – $2.5 M_{\odot}$ ) which are dwarfs or giants of

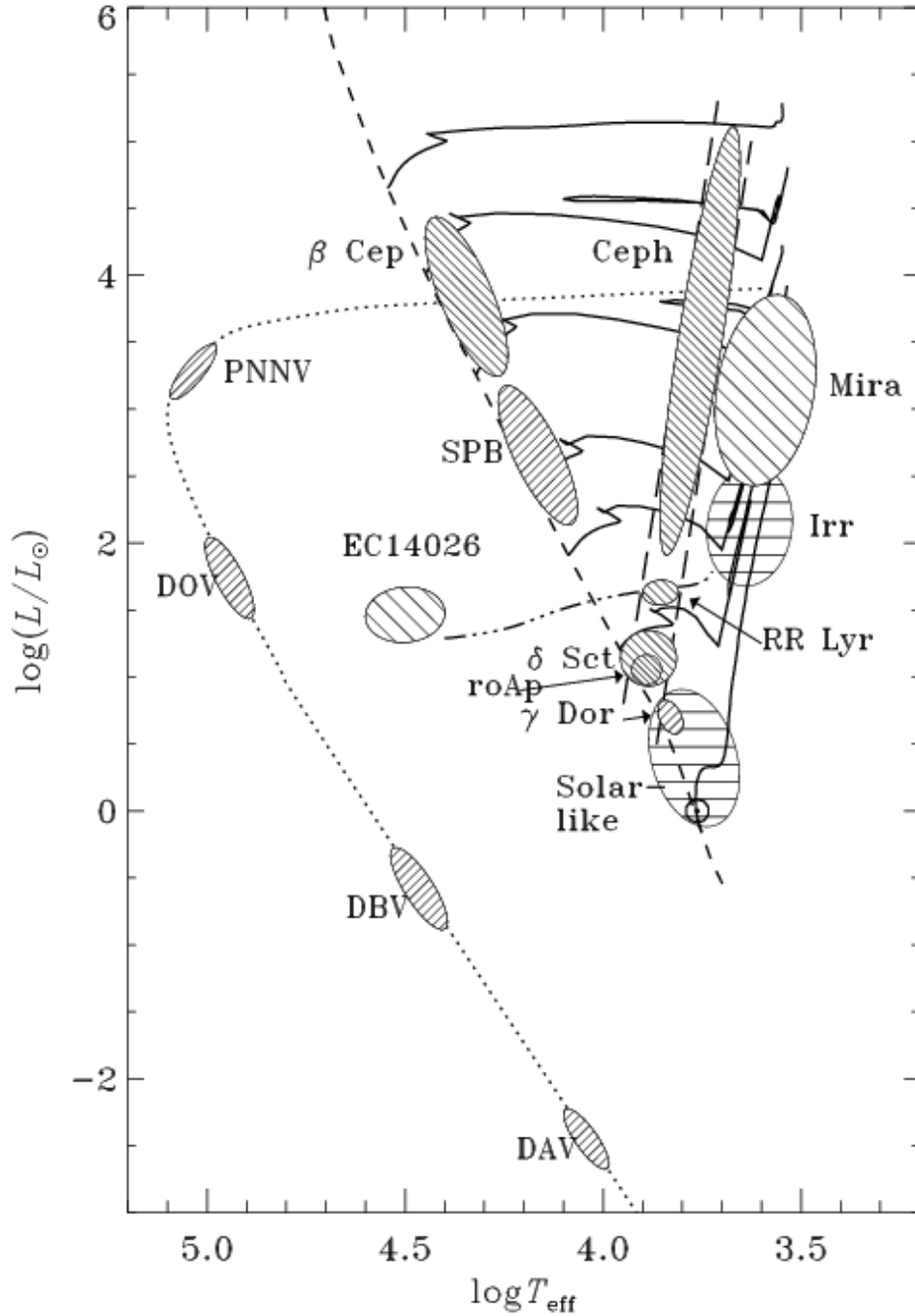


Figure 1 : Theoretical HR diagram schematically illustrating locations of known pulsating stars. The dashed line marks the zero-age main sequence (ZAMS) where the solar-like oscillators,  $\gamma$  Doradus,  $\delta$  Scuti and  $\text{roAp}$  stars are located. The dotted line corresponds to the cooling sequence of white dwarfs, where one finds active planetary-nebula nuclei variable, variable white dwarfs. The parallel long-dashed lines indicate the Cepheid instability strip where RR Lyrae and Cepheids are situated. Adapted from Christensen-Dalsgaard (2000).

spectral type A2–F5 located in the extension of the Cepheid instability strip and pulsate with period of 0.02–0.3 d. Chemically peculiar (CP) pulsating magnetic stars of spectral type A are known as rapidly oscillating Ap (roAp) pulsators with period between  $\sim 5$ –23 min. Among the F-type stars there are the  $\gamma$  Dor pulsators ( $M \sim 1.4$ – $1.6 M_{\odot}$ ) that pulsate with periods 0.3–3 d. At ARIES we have been studying the MS pulsating stars asteroseismically and participate in whole earth telescope (WET) campaigns organized for the un-interrupted time-series observations of pulsating variables.

#### 4. Basic Properties of Stellar Oscillations

Generally stellar oscillations are studied in the linear regime where one considers small displacements. Owing to limitations on existing computers, non-linear regime can only be studied for radial pulsations where the equations are greatly simplified. As a result we can predict the oscillation frequencies for any given stellar model but not the amplitude of the pulsations.

The small amplitude, linear oscillations of a spherically symmetric non-rotating star can be expressed in terms of a spherical harmonic  $Y_l^m(\theta, \phi)$  where  $\theta$  is co-latitude and  $\phi$  is the longitude. The radial component of displacement can be expressed as :

$$\xi_r(r, \theta, \phi; t) = \Re \{ a(r) Y_l^m(\theta, \phi) \exp(-i 2\pi \nu t) \} , \quad (2)$$

where  $r$  is the distance to the center of the star,  $a(r)$  is an amplitude function and  $\nu$  is the cyclic frequency of the oscillation. For a spherically symmetric star the frequency of oscillations depend on  $n$  and  $l$ , i.e.,  $\nu = \nu_{nl}$ .

The spherical harmonic  $Y_l^m(\theta, \phi)$  is expressed as :

$$Y_l^m(\theta, \phi) = (-1)^m c_{lm} P_l^m(\cos \theta) \exp(i m \phi) , \quad (3)$$

where  $P_l^m$  is an associated Legendre function given by

$$P_l^m(\cos \theta) = \frac{1}{2^l l!} (1 - \cos^2 \theta)^{m/2} \frac{d^{l+m}}{d \cos^{l+m} \theta} (\cos^2 \theta - 1)^l , \quad (4)$$

and the normalization constant  $c_{lm}$  is determined by

$$c_{lm}^2 = \frac{(2l+1)(l-m)!}{4\pi(l+m)!} , \quad (5)$$

such that the integral of  $|Y_l^m|^2$  over the unit sphere is unity.

Each eigenmode of a spherically symmetric star is specified by the three indices,  $n, l$  and  $m$ , which are called the radial order, the spherical degree and the azimuthal order, respectively. The radial order  $n$  is associated with the structure in the radial direction, the indices  $l$  represents the number of the surface nodes or lines in the direction of equator and  $m$  defines the

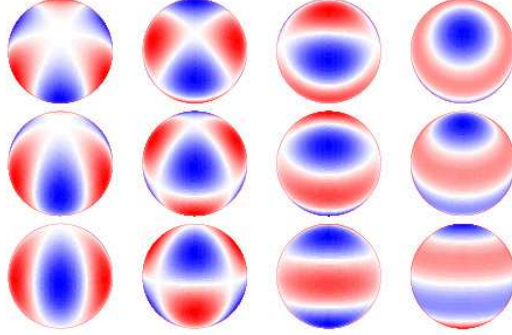


Figure 2 : Snapshot of the radial component of the  $l = 3$  octupole modes. Each row display the same modes with different inclination angles of the polar axis with respect to the line of sight:  $30^\circ$  (top row),  $60^\circ$  (middle row), and  $90^\circ$  (bottom row). White bands represent the nodal surface lines, red and blue sections represent portions of the stellar surface that are moving in and out, respectively. The right-most column displays the axisymmetric (i.e., with  $m = 0$ ) mode ( $l = 3, m = 0$ ). From right to left, the middle columns display the tesseral (i.e., with  $0 < |m| < l$ ) modes ( $l = 3, m = \pm 1$ ) and ( $l = 3, m = \pm 2$ ). The left-most column displays the sectoral (i.e., with  $|m|=l$ ) mode ( $l=3, m = \pm 3$ ). Adopted from Kurtz et al. (2006).

number of surface nodes that are lines of longitude (Takata 2012). The modes with  $l=0, 1$  and  $2$  correspond to radial, dipolar and quadrupole-polar modes, respectively. The modes with  $m \neq 0$  are traveling waves. Modes traveling in the direction of rotation are called prograde modes (positive  $m$ ) while waves traveling in the opposite direction are called retrograde modes (negative  $m$ ). Low-overtone modes have  $n < 5$  and high-overtone modes have  $n > 20$ . Fig. 2 illustrates the appearance of the  $l=3$  octupole modes on a stellar surface.

There are  $2l + 1$  values of  $m$  for each value of degree  $l$ . In the case of a spherically symmetric, non-rotating star their frequencies will be the same. Rotation, as well as any other physical process results in a departure from spherical symmetry that introduces a dependence of the frequencies of non-radial modes on  $m$ . When the cyclic rotational frequency of the star,  $\nu_{rot}$  is small and in the case of rigid-body rotation, the cyclic frequency of a non-radial mode is given to first order (Ledoux 1951):

$$\nu_{nlm} = \nu_{nl0} + m\nu_{rot}, |m| \leq l \quad (6)$$

High-degree modes penetrate only to a shallow depth while low-degree modes penetrate more deeply. If many modes are present then a range of depths can be investigated. It is then possible to “invert” the observations to



make a map of the sound speed throughout the star. One may thus deduce the temperature and density profile using reasonable assumptions about the chemical composition.

In a non-radial mode, some parts of the stellar surface are brighter and others fainter. Some parts are moving towards the observer and others away from the observer. As a result, the nullifying effect reduces the observed light and radial velocity amplitude. The higher the value of  $l$ , the greater the nullifying effect. For most stars observed from the ground, only modes with  $l < 4$  are typically detectable.

#### 4.1 Pressure and Gravity Modes

There are two main sets of solutions of the equations of motion for a pulsating star leading to two types of pulsation modes namely  $p$ - and  $g$ -modes. For the  $p$ - or pressure modes, pressure acts as the restoring force for a star perturbed from equilibrium. The  $p$ -modes are acoustic waves and have motions that are primarily vertical. For the  $g$ - or gravity modes buoyancy acts as a restoring force and gas motions are primarily horizontal.

There are two other important properties of  $p$ -modes and  $g$ -modes: (1) as the radial overtone ( $n$ ) increases, the frequencies of the  $p$  modes increase, but the frequencies of the  $g$ -modes decrease; (2) the  $p$ -modes are sensitive to conditions in the outer part of the star, whereas  $g$ -modes are sensitive to the core conditions. Since buoyancy demands motions that are primarily horizontal, there are no radial (i.e.,  $l = 0$ )  $g$ -modes. As stars evolve, the convective envelope expands and the acoustic oscillation modes ( $p$ -modes) decrease in frequency. At the same time,  $g$ -mode oscillations that exist in the core of the star increase in frequency as the core becomes more centrally condensed. Eventually,  $p$ - and  $g$ -mode frequencies overlap, resulting in oscillation modes that have a mixed character, behaving like  $g$ -modes in the core and  $p$ -modes in the envelope.

To identify the  $p$ -mode radial overtones, it is useful to introduce a quantity known as the pulsation constant  $Q$  defined as :

$$Q = P_{\text{osc}} \sqrt{\frac{\bar{\rho}}{\bar{\rho}_{\odot}}} \quad (7)$$

where  $P_{\text{osc}}$  is the pulsation period and  $\bar{\rho}$  is the mean density of the star.

Equation (7) can be rewritten as

$$\log Q = -6.454 + \log P_{\text{osc}} + \frac{1}{2} \log g + \frac{1}{10} M_{\text{bol}} + \log T_{\text{eff}}, \quad (8)$$

where the unit of  $P_{\text{osc}}$ ,  $\log g$  and  $T_{\text{eff}}$  are in unit of days, dex and Kelvin, respectively. Table 2 lists the value of  $Q$  for a  $\delta$  Scuti star pulsating in different modes. The value of  $Q$  is not too sensitive to  $M_{\text{bol}}$  or  $T_{\text{eff}}$ , but it is

sensitive to  $\log g$ , which is the most uncertain quantity. For standard late-A and early-F star models, we expect  $Q=0.033$  and  $Q=0.025$  for the fundamental and first-overtone mode (Stellingwerf 1979), respectively. Breger & Bregman (1975) demonstrated that for  $T_{\text{eff}} < 7800$  K, the highest amplitude mode tends to be the fundamental mode, whereas for hotter temperatures the first overtone is prevalent.

#### 4.1.1 The Asymptotic Relation

If the condition  $l \ll n$  is satisfied, the excited  $p$ -modes in a non-rotating star can be described according to the asymptotic theory (Tassoul 1980), which predicts that oscillation frequencies  $\nu_{n,l}$  of acoustic modes, characterized by radial order ( $n$ ) and harmonic degree ( $l$ ) satisfy the following approximation:

$$\nu_{nl} \approx \Delta\nu\left(n + \frac{1}{2}l + \epsilon\right) - \delta\nu_{n,l} \quad (9)$$

where  $\epsilon$  is a constant sensitive to the surface layers. From observational point of view it is convenient to represent the frequency spectrum by the average quantities  $\Delta\nu = \nu_{n,l} - \nu_{n-1,l}$  and  $\delta\nu_{n,l} = \nu_{n+1,l} - \nu_{n,l}$

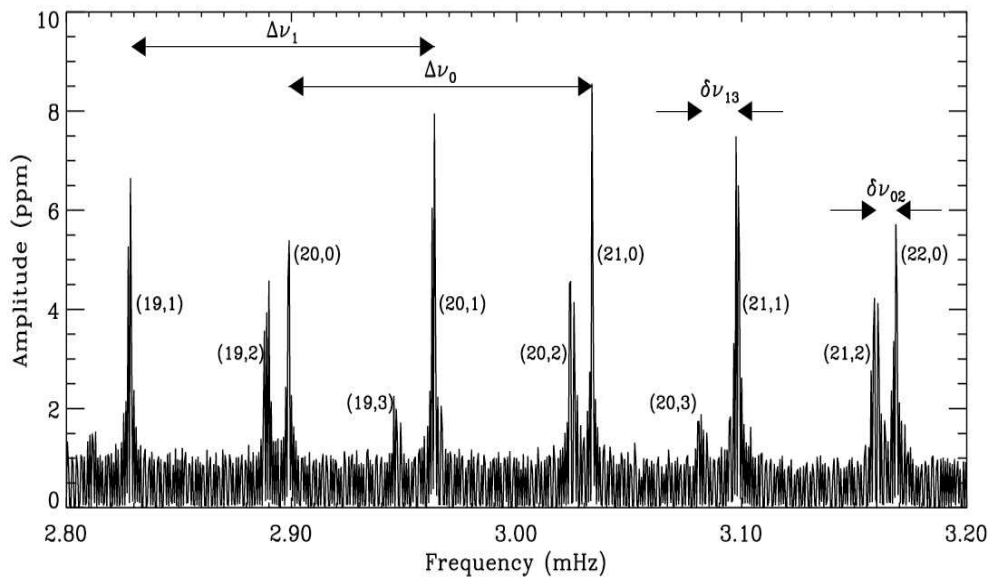
The parameter  $\Delta\nu$  which is the frequency difference between successive modes of the same  $l$  is called the *large separation*. This is proportional to the inverse of the sound travel time across the stellar diameter. This is related to the sound speed profile in the star and proportional to the square root of the mean density of the star :

$$\Delta\nu_0 = \left(2 \int_0^R \frac{dr}{c}\right)^{-1} \propto \sqrt{\bar{\rho}} \quad (10)$$

where  $c$  is sound speed,  $\bar{\rho}$  is mean density and  $R$  is the stellar radius. The parameter  $\delta\nu_{n,l}$  is known as the *small separation* and is sensitive to the core region of the star which in turn is sensitive to the composition profile. Thus the small frequency separation is an important diagnostic of the stellar evolution. The large and the small separations in the acoustic amplitude spectrum of the Sun is shown in Fig. 3.

Measuring the large and small separations gives a measure of the mean density and evolutionary state of the star. A useful seismic diagnostic is the asteroseismic HR diagram where the average large separation is plotted against its average small separation and known as the ‘‘C-D’’ diagram (Christensen-Dalsgaard 1984). Fig. 4 shows the C-D diagram for models with near-solar metallicity. The solid lines show the evolution of  $\Delta\nu$  and  $\delta\nu_{02}$  for models with a metallicity close to solar and various masses. Isochrones of different age are also shown with dashed lines. For MS, the asteroseismic C-D diagram allows us to estimate the mass and age of the star assuming that other physical inputs such as initial chemical composition and the convective mixing-length parameter are known. As stars evolve off

Figure 3 : Close-up of the  $p$ -mode amplitude spectrum of the Sun. The peaks are marked with the corresponding  $(n, l)$  values, which were determined by comparison with theoretical models. Adopted from Bedding & Kjeldsen (2003).



the MS, their tracks converge for the sub-giant and red-giant evolutionary stages.

The high-order  $g$ -modes are observed in  $\gamma$ -Dor and SPB stars as well as in white dwarfs. In the absence of rotation, the periods  $\Pi_{n,l}=1/\nu_{n,l}$  are approximately uniformly spaced and to first order satisfy the relation :

$$\Pi_{n,l} = \frac{\Pi_0(n + \frac{l}{2} + \alpha_g)}{\sqrt{l(l+1)}} \quad (11)$$

where  $\Pi_0 = 2\pi^2 \left( \int_{r_1}^{r_2} \frac{N}{r} dr \right)^{-1}$  is the basic period spacing,  $N$  is the buoyancy (or Brunt-Vaisala) frequency and  $[r_1, r_2]$  is the interval where the modes are trapped.  $\alpha$  is a phase constant that depends on the details of the boundaries of the  $g$ -mode trapping region and the integral is computed over that same region. Departures from the simple asymptotic relation given in Eq. 11 is used as a means to diagnose the stratification inside stars such as white dwarfs.

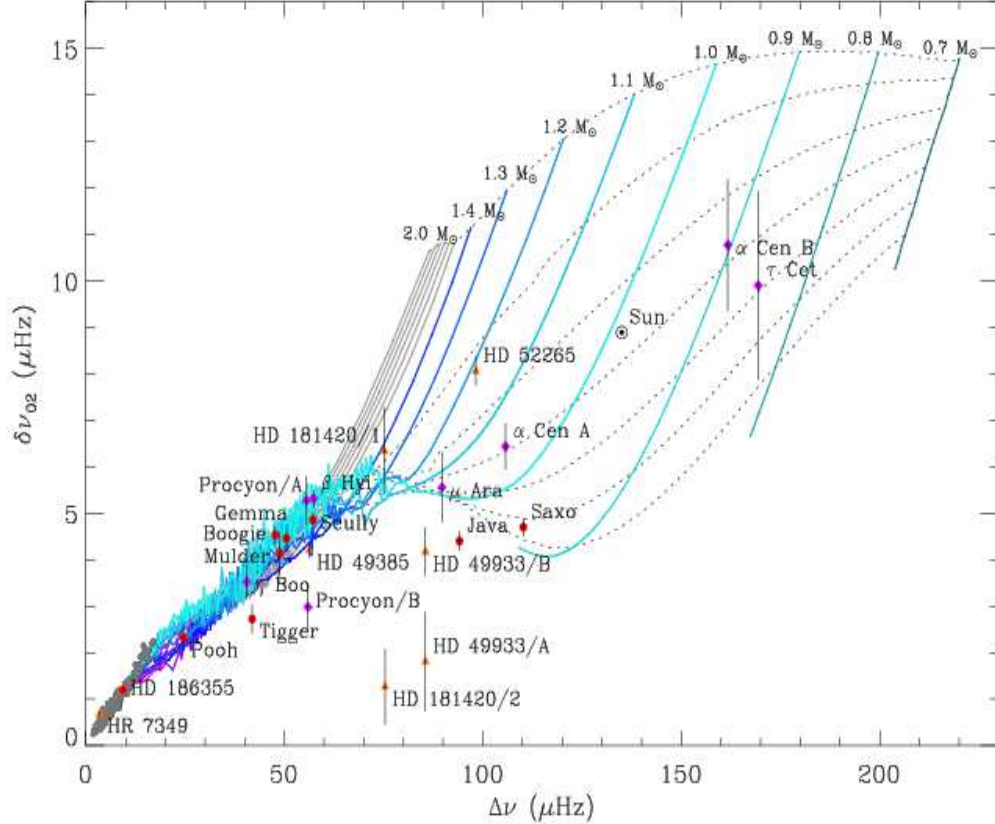


Figure 4 : C-D digram showing the large separation versus the small separation for a series of evolution models calculated for different masses with model tracks for near-solar metallicity ( $Z_0 = 0.017$ ). The section of the evolutionary tracks in which the models have a higher  $T_{eff}$  than the approximate cool edge of the classical instability strip (Saio & Gautschy 1998) are gray. Dashed black lines are isochrones, increasing by 2 Gyr from 0 Gyr (ZAMS) at the top to 12 Gyr at the bottom. Stars observed by CoRoT (orange triangles), Kepler (red circles) and from the ground (purple diamonds) are marked. Gray circles are Kepler red giants (Huber et al. 2010) and Sun is marked by its usual symbol. Adopted from White et al. (2011).

#### 4.2 Identification of Pulsation Modes

Successful seismic modeling involves not only detection of pulsation frequencies but also relies on the identification of the spherical harmonic numbers ( $n, l, m$ ) of the observed modes. Two particularly promising methods for identifying pulsation modes are multi-colour photometric and spectroscopic

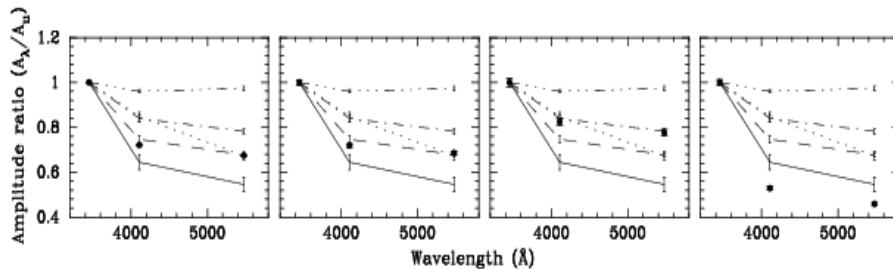


Figure 5 : Identification of the four strongest pulsation modes of the  $\beta$  Cephei star 12 Lacertae using multi-colour photometry. Adopted from Handler et al. (2006).

mode identification. The first approach consists of measuring the amplitudes and phases of a given pulsation mode in different photometric bands, calculating the ratios of the different amplitudes and/or the phase differences, and comparing to theoretical predictions. The value of  $l$  can be determined from the amplitude ratios and phase differences of the variation at different wavelength bands (Garrido et al. 1990). The second approach exploits the Doppler shifts caused by the velocity field from the pulsation mode and how it affects observed absorption lines. These methods have been successfully applied to slowly rotating stars (e.g. De Ridder et al. 2004; Zima et al. 2006; Briquet et al. 2007), but more work is required before they are applied to rapid rotators. High-resolution spectroscopy can be used to study the line profile variations (LPVs) during the pulsation. The observed profile variations are compared with the profile variations modeled for different values of  $l$  and  $m$ .

Photometric mode identification is widely used because it is very effective and easy to use if the observations are sufficiently precise. The amplitude ratios can be calculated following the method of Dupret et al. (2003) and an example of such a mode identification is shown in Fig. 5. The spectroscopic method of mode identification relies on the Doppler effect. The intrinsic line profile is blue-shifted in the parts of the stellar surface approaching the observer and red-shifted on those parts moving away from the observer. The effect is strongest on the stellar limb and decreases towards the center. Hence, a rotationally broadened line profile contains spatial information of the brightness distribution on the stellar surface such as that caused by stellar pulsation. The method of reconstructing the stellar surface brightness distribution from line profile variations is called Doppler Imaging (Telting 2003). By examining a stellar line profile pulsation modes up to  $l \approx 20$  can

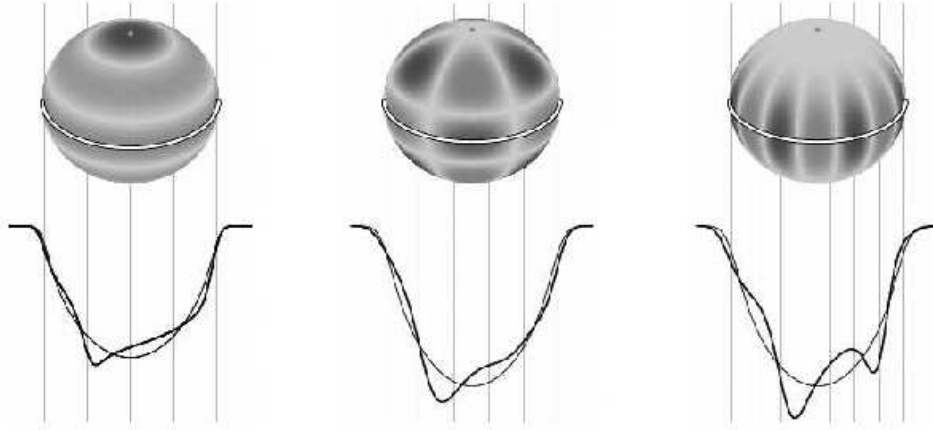


Figure 6 : Line profile variations due to stellar pulsation. The upper parts of the graph shows the shape of the oscillation mode on the surface, whereas the thin lines in the lower halves represent the unperturbed rotationally broadened line profile, and the thick lines are the superpositions with the pulsation. Each individual mode (from left to right:  $l = 4, m = 0$ ;  $l = 5, |m| = 3$ ;  $l = |m| = 7$ ) generates a different distortion of the line profile. Adopted from Telting & Schrijvers (1997).

be observed and identified. One example of pulsational line profile variations is shown in Fig. 6.

High-resolution spectroscopy allows us to study LPVs using different methods. To study the LPVs from the spectroscopic data one should carefully select a number of unblended, deep lines and avoid saturated lines. Averaging all lines in the spectrum (Uytterhoeven et al. 2008) provides high S/N mean line profile. This can be done using cross-correlation. The drawback of the spectroscopic method is that it assumes that all the lines have the same intrinsic profile and that they form in the same region of the atmosphere, which may not be the case. In spite of the fact that high-dispersion spectroscopy potentially contains more information than multi-colour photometry, most mode identifications are performed from multi-colour photometry. Spectroscopy is mostly used for the confirmation of the mode identified using photometry (Daszyńska-Daszkiewicz et al. 2005).

More recently Lignières & Georgeot (2009) calculated geometrical disk integration factors of acoustic modes in deformed polytropic models by integrating the temperature fluctuations over the visible disk. The effects of rotation were fully taken into account in the pulsation modes, thanks to the

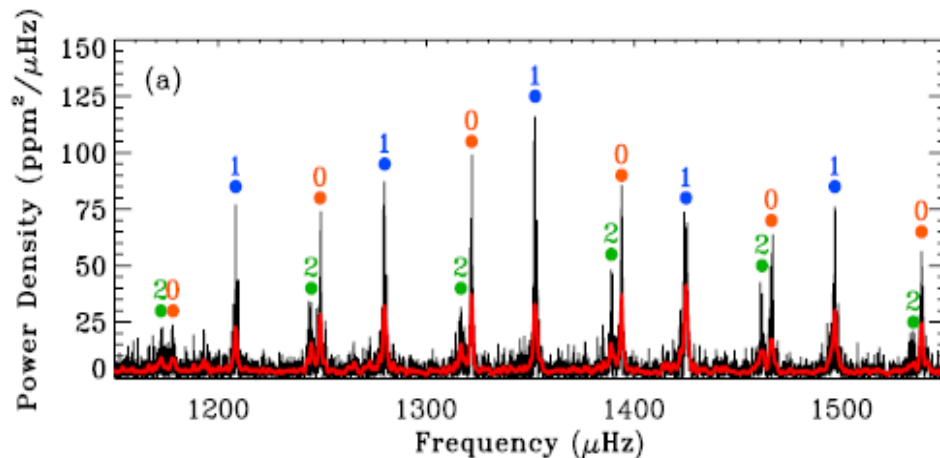


Figure 7 : Power spectra of a G-type star KIC 6933899. The red curves show the power spectra after smoothing. Mode identification of the G star is trivial, with modes of  $l = 0$  (orange), 1 (blue), and 2 (green) labeled. Adopted from White et al. (2012).

2-D numerical approach, but non-adiabatic effects were neglected, thereby making the fluctuations of the effective temperature inaccessible.

In the Sun and solar-like oscillators the mode identification is straightforward thanks to the distinctive pattern of alternating odd and even modes in the power spectrum. Each  $l = 0$  mode is separated by  $\delta\nu_{02}$  from an  $l = 2$ , and separated by  $\Delta\nu/2 - \delta\nu_{01}$  from the  $l = 1$  mode of the same order. An example is shown in Fig. 7 for the Kepler star KIC 6933899 of effective temperature of 5840 K similar to the Sun (White et al. 2012). Fig. 3 shows the identification of the modes from the solar spectrum.

The échelle diagram can be used to identify the angular degree of an observed frequency. This process was first suggested by Grec et al. (1983) and used to identify the degree of solar modes. The process involves splitting a spectrum into lengths of the stars large separation which are then stacked on top of each other. This process has the effect of lining up frequencies into ridges corresponding to different angular degrees. Fig. 8 shows an example of an échelle plot created from frequencies found in data collected by BiSON network. In this figure we can see that the frequencies are splitted into four distinct regions.

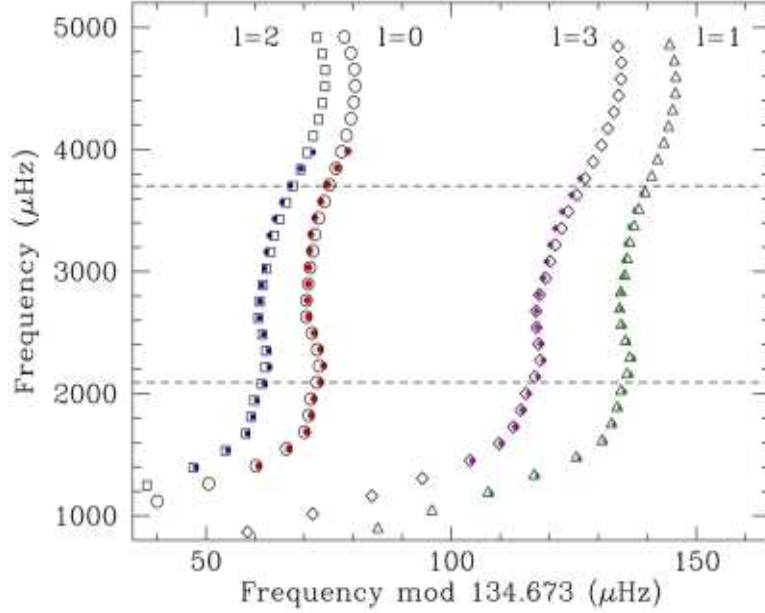


Figure 8 : An échelle diagram for the Sun observed as a star, where we divide the oscillation spectrum into segments of a fixed length and plot them against the oscillation frequency. Colored symbols show the observations while open points show the best stellar model. From left to right the ridges are paired  $l = 2$  then  $l = 0$ . Followed by the odd pair of  $l = 3$  and  $l = 0$ . Adopted from Metcalf et al. (2009).

## 5. Pulsational Mechanism

The mechanism which drives stellar oscillations can be inferred by studying and modeling the energy transport in the interior of a star. We have mentioned three types of oscillating star: stars exhibiting solar-like oscillations (including the Sun itself), Cepheid variables and Mira. Pulsations in these three different types of stars are driven by different excitation mechanisms.

Self-driven oscillations, such as those in Cepheid variables, can be either intrinsically unstable or intrinsically stable depending upon the mechanism. In the former case, oscillations result from the amplification of small disturbances by means of a heat-engine or valve mechanism converting thermal energy into mechanical energy in a specific region usually a radial layer of the star (Zhevakin 1963). During the compression phase heat is absorbed, while in the expansion phase heat is released. In order to cause overall excitation of the oscillations, the region associated with the driving has to be at an appropriate depth inside the star, thus providing an explanation for the specific location of the resulting instability belt in the H-R diagram



(Fig. 1). Such a region is typically associated with a region of ionization of an abundant elements. Normally, the opacity decreases as the temperature increases. In most regions of a star, compression results in an increase in temperature. The resulting decrease in opacity contributes strongly to heat leakage and to the stability of the star as a whole. However, in a zone where an abundant atomic species is partly ionized, the opacity increases with temperature because radiation is absorbed by ionization of the material. Upon compression, some of the heat is absorbed in ionizing more of the atomic species. Thus energy is absorbed on compression and released on expansion. The cycle repeats and this process is known as the  $\kappa$ -mechanism. It is believe that  $\kappa$ -mechanism is responsible for the pulsations observed in stars that are located on the instability strip: classical Cepheids, WW Virginis, RR Lyrae and  $\delta$  Scuti stars. The pulsation mechanism for other stars outside the instability strip such as Miras, semi-regular variables is not so well understood.

Solar-like oscillations are expected in cool main-sequence, sub-giant and red-giant stars ( $0.1M_{\odot} < M < 8M_{\odot}$  (Christensen-Dalsgaard & Frandsen 1983; Houdek et al. 1999; Chaplin et al. 2011a,b; Hekker et al. 2011; Chaplin & Miglio 2013)). It is popularly accepted that the five-minutes oscillations of the Sun are excited by the stochastic effect of turbulence (Goldreich & Keeley 1977; Kumar & Goldreich 1989; Goldreich et al. 1994; Belkacem et al. 2008). As a natural extension, solar-like oscillations of stars have also been considered to be due to the same stochastic excitation of turbulence (Samadi & Goupil 2001; Samadi et al. 2003; Samadi et al. 2008).

## 6. Measurements of Variability

Stellar oscillations generate motions and temperature variations causes light, radial velocity and line profile changes. Pulsating stars can be studied both photometrically and spectroscopically, via time-series measurements. The angular diameters of stars are too small to resolve surface features and we must rely on integrated light or radial velocity variations of the visible hemisphere of the star. In the following sub-sections we briefly describe only two methods of obtaining asteroseismic information.

### 6.1 Photometric Technique

The integrated stellar intensity can be measured using photoelectric and CCD photometry. The field of view allows the simultaneous observation of many stars. The major source of atmospheric noise in photometric observations is sky transparency variations. On a photometric night the sky transparency variations occur on times-scale of about 15-min and longer giving rise to low-frequency noise. This noise can be be partially controlled

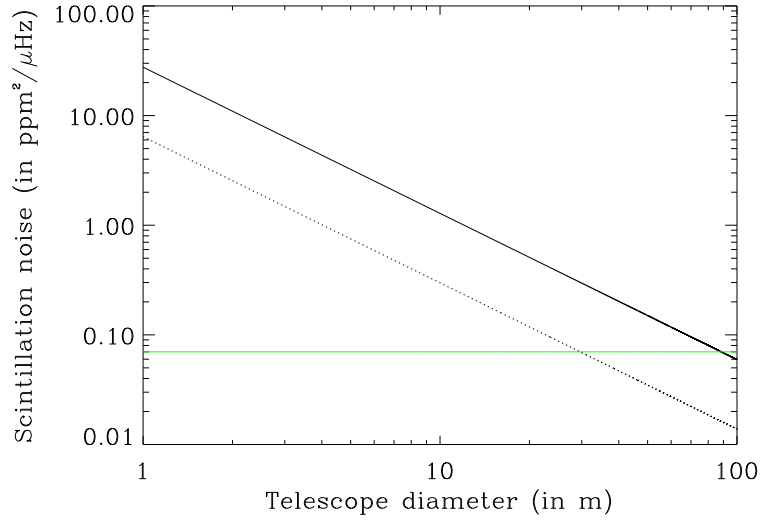


Figure 9 : Scintillation noise as a function of telescope diameter for an air-mass of  $X = 1.5$  (solid line) and of  $X = 1.0$  (dotted line) for an observatory located at altitude of 4000 m. The green line is the limit of the scintillation noise for the solar-like oscillations. Adopted from Appourchaux & Grundahl (2013).

by observation of non-variable comparison stars or observing a star under photometric sky condition. The second major source of atmospheric noise in photometry is scintillation caused by variable refraction. In practice, scintillation noise drops inversely with telescope aperture (Dravins et al. 1998). Fig. 9 shows the variation of the scintillation noise with the diameter of telescope which clearly reveals that the scintillation noise can be reduced by observing with a bigger telescope.

## 6.2 Spectroscopic Technique

The measurement of radial velocity (RV) from a single absorption line is a challenging task because of the lack of photons. Therefore, the spectrograph should cover a wide wavelength range at high-resolution with minimum optical loss. The spectrographs such as High Accuracy Radial Velocity Planet Searcher (HARPS) achieve high-spectral stability by controlling of the air pressure and temperature in the instrument (Pepe et al. 2000). The precision reached by such an instrument depends primarily on the number of photons gathered (telescope diameter, optical efficiency); the spectral coverage and the resolving power.

An added benefit of RV compared to light intensity measurements is that the canceling effect for non-radial oscillations is smaller, allowing modes of high  $l$  to be observed and to detect modes of life times up-to a year (Salabert et al. 2009). A combination of spectroscopic and photometric observations, preferably simultaneously is of great importance for correct interpretation of the data. Such studies allow to determine the phase lag between light and RV curves, an important parameter for modeling of stellar structure. Intense observing campaigns that combined ground based spectroscopy and space-based photometry obtained with the MOST satellite were organized for the asteroseismic study of roAp stars HD 24712 (Ryabchikova et al. 2007), 10 Aql (Sachkov et al. 2008) and 33 Lib (Sachkov et al. 2011).

## 7. Ground and Space based Observations

Different types of data sets and techniques are used for asteroseismology. A few milestones that have occurred in the past few years are: 1) Small and medium-sized telescopes all over the world have been collecting optical photometry with photoelectric photometers and CCDs detectors; 2) co-ordinated multi-site campaigns such as WET set-up by different communities have been used to obtain the continuous observations. These networks have improved the precision of the frequencies of pulsation by minimizing the aliasing; 3) in the past few years the development of high-accuracy spectrographs such as HARPS and Ultraviolet and Visual Echelle Spectrograph (UVES) have allowed the detection and eventually confirm the presence of solar-like oscillations in stars other than Sun. These efforts have contributed to the refinement of global parameters of stars and provided the mode identification; 4) large surveys such as Optical Gravitational Lensing Experiment (*OGLE*) and Massive Compact Halo Object (*MACHO*) have detected numerous pulsating variables; and 5) Interferometers such as Center for High Angular Resolution Astrometry (*CHARA*) and Very Large Telescope Interferometer (*VLTI*) have contributed significantly in asteroseismology in terms of providing accurate radii for the pulsating variables.

The precision obtained from ground-based photometric observations is not sufficient to detect the  $\mu$ -mag amplitudes of the solar-like oscillations. From space, much lower detection levels were first obtained on whole-disk observations of the Sun (Woodard & Hudson 1983). The space-based instruments such as *Wide Field Infrared Explorer (WIRE)* (Buzasi et al. 2000), *MOST* (Matthews et al. 2004) discovered many stars exhibiting the solar-like oscillations. Asteroseismic space missions have revolutionized the field asteroseismology with the launch of *CoRoT* (Michel et al. 2008; Auvergne et al. 2009; Baglin et al. 2009) and *Kepler* (Chaplin et al. 2010, Koch et al. 2010). The primary aim of both the missions were detection of ex-

oplanets using the transit technique with secondary purpose to make the asteroseismic studies of pulsating variables.

The CoRoT satellite was launched on 27 December 2006 into an orbit around the Earth. This satellite had an off-axis telescope of diameter of 28 cm. Four CCD detectors are mounted at the focal plane, covering  $1.3^\circ \times 1.3^\circ$  field of view for each CCD. Two of the CCDs are optimized for studying planet transits and the other two, with slightly defocused images, optimized for asteroseismology. The detection of solar-like oscillations in hundreds of red giants was a landmark for the CoRoT mission (De Ridder et al. 2009).

The *Kepler* mission was launched on 7 March 2009 into an Earth-trailing heliocentric orbit for a period of around 53 weeks and still operational. *Kepler* observed a fixed field in the region of the constellations of Cygnus and Lyra, centered  $13.5^\circ$  above the Galactic plane. *Kepler* has a Schmidt telescope with a corrector diameter 0.95-m. Array of 42 CCD array with a total of 95 megapixels covers a field of around 105 square degrees. The brightness variation on up to 170,000 targets were available in the 29.4-minute long cadence (LC) almost continuously over four years. A total of 512 main sequence and giants stars were observed with a 58.85-sec cadence over a time span of a few months. Chaplin et al. (2014) have presented a homogeneous asteroseismic analysis of more than 500 stars and derived their global asteroseismic parameters.

Temporal coverage has a strong impact on detection of stellar variability. Gaps in the time-series data are obvious due to bad weather conditions and to day/night breaks. Mosser & Aristidi (2007) showed that since the local time approximately shifts by 4 min per day with respect to the sidereal time, the duration of an observation run on the same star cannot be longer than 5 months. The small temporal data due to interruptions generate daily aliases in the frequency spectrum located at  $11.57 \mu\text{Hz}$  and its harmonics. These aliases make mode identification difficult when the frequency separation is about that value. It is often suggested that the presence of such interruptions could be avoided by observing pulsating variables with a network of telescopes spread around the globe. This applies to both stellar radial velocity and photometric measurements. The helioseismic ground-based networks that have been operating for last three decades are GONG (Harvey et al. 1996) and BiSON (Chaplin et al. 1996)). Similarly the ground-based networks such as WET uses many telescopes all over the world.

The advantage of a space mission over ground-based observations is mainly in the high precision and large sky coverage that can be achieved for long durations without any interruption. Another advantage of space observations is the possibility of using wavebands which are blocked by the atmosphere (UV, EUV, X rays).

The advantage of the ground-based spectroscopic observations is that it is possible to detect oscillation frequencies to much higher precision and at lower frequencies with radial-velocity observations. Furthermore, it is

possible to detect  $l > 3$  modes through line profile measurements. The ground-based photometric observations can be used for mode identification which require multi-band observations currently not available from space. The overwhelming advantage of ground-based observations, of course, is that they are inexpensive. A single space mission costs far more than a large telescope and can cover operating expenses of ground-based observations for many years.

## 8. Asteroseismic Techniques

The determination of the pulsation frequencies is the first objective in any asteroseismic investigation, accomplished by constructing the periodogram which is the Fourier transform of time-series data that gives the power or amplitude as a function of time. The oscillation frequencies are seen as sharp peaks in the periodogram which can be easily identified if the height of the peak is much larger than the background noise level in the periodogram.

For the frequency analysis of the classical pulsators traditionally, a process called “pre-whitening” is used to extract the frequencies from the periodogram and particularly it is useful to remove the unwanted frequency peaks which otherwise arise due to aliases or earth atmosphere. This consists in identifying the frequency of a peak and removing a sinusoid with this frequency and to determine correct amplitude and phase from the data. A periodogram of the pre-whitened data no longer shows a peak at this frequency. The process of successive pre-whitening stops when the peak of highest-amplitude in the periodogram has an amplitude which is considered too small to be significant. A widespread criterion used for this purpose is to calculate the ratio of the peak amplitude to the background noise level. When the S/N ratio is less than 4, the signal is no longer considered statistically significant (Breger et al. 1993).

This technique works well for ground-based data where the S/N is quite moderate. For space observations of very high S/N, the prewhitening technique introduces additional low-amplitude side-lobes due to inevitable errors in frequency determination. For example the periodogram of solar-like oscillations exhibits the comb-like structure with amplitudes which decrease sharply from a central maximum and in such case to identify the location of the frequency of maximum amplitude ( $\nu_{max}$ ) is very important. A crude way of obtaining  $\nu_{max}$  is to simply look at the periodogram and estimate the frequency of maximum amplitude of the Gaussian envelope of the peaks (Balona 2014).

High-speed photometry is widely used in asteroseismology, particularly for the high-frequency pulsations present in white dwarfs, sdBV and roAp stars. High-speed photometry does not refer to high-time resolution, but rather that the target star varies more rapidly than the time for an observer

to move the telescope between the target and comparison stars. In such a situation one should continuously observe the target star instead of observing the comparison stars. This technique is also known as non-differential photometry. To study stellar pulsation it is necessary to use integration time shorter than the pulsation period so that one can collect as many as data points over one pulsation cycle. Photometric integration times for asteroseismic targets are often selected to be 10-sec, and may be averaged to longer integrations. Differential photometry is the standard method for all photometric asteroseismic observations. In differential photometry it is always desirable to observe one or two non-variable comparison stars of similar magnitude and color close to the target star to correct for the sky transparency variations.

Ground-based photometry normally consists of many CCD exposures of the target field. The raw CCD data needs to be corrected for bias and flat fielding. Synthetic aperture photometry of the target star and several comparison stars in the same CCD frame are used to calculate the relative brightness of the target with respect to comparison stars. Sometimes it is possible to increase the photometric accuracy by using profile fitting to the stellar images on the CCD instead of aperture photometry (Stetson 1987). Profile fitting gives superior results in crowded fields or for very faint objects.

Spectroscopic observations of pulsating stars can provide additional information particularly for the determination of the projected rotational velocity,  $v \sin i$ . Surface rotation can also be used as an observable to determine the age of the star. Spectroscopic studies of hundreds of stars in each spectral type from O to M has shown over the years that the early-type stars of classes O, B and A have rotational velocities between 200 and 350 km/sec, and that at spectral type F, there is a rapid decline from about 100 km/sec at F0 to 10 km/sec at G0. The Sun, a G2 star rotates at about 2 km/sec, and red giants rotate at 1 km/sec and slower. Since stellar rotation slows with age, hence the rotation period of any star can be used to derive its age – a technique referred to as “gyrochronology” which is an empirical relationship between rotation period, color, and age (Chaname & Ramirez 2012). It provides means by which surface rotation can be used to infer ages of cool stars (e.g. Barnes 2009). The rotation-age relationship can be established but also for stars like our Sun.

Stars are rotating and their rotation affects their oscillation frequencies. The information is relatively easy to conclude that the star rotates slowly provided observations are of superior quality that allows us to achieve the necessary high-accuracy of frequency measurements. On the other hand, when the star is rotating fast, one should properly take into account the consequences of the spheroidal shape of the star on the oscillation frequencies before extracting seismological information on the internal structure or the rotation profile of the star. The asymptotic relations works well when the

rotation is small and the measurements of the rotational splittings is used to determine the internal rotation velocity.

Solar-type stars are generally slow rotators (in most cases  $v \sin i < 20$  km/sec) and the influence of rotation on the oscillation frequencies is well known. However, distortion due to the centrifugal force can have a large impact on the oscillation frequencies even for slow rotators (e.g. Goupil 2009; Reese 2010, and references therein). Such an effect is stronger for acoustic ( $p$ ) modes with small inertia, which have a higher sensitivity to the outer layers of the star. Therefore, their frequencies are more sensitive to the physical properties of the surface, where the centrifugal force becomes more efficient (Suárez et al. 2010; Ouazzani & Goupil 2012). Much more evolved star such as a Cepheid is a radially pulsating star and a slow rotator. However period ratios of radial modes can be quite significantly affected by rotation as mentioned by Pamyatnykh (2003, Fig.6) for a  $\delta$  Scuti star and quantified by Suárez et al. (2007) for a Cepheid. For hotter stars, rotation is more rapid and it is no longer possible to use the asymptotic relation. In fact, rotation is the most serious obstacle to the interpretation of pulsating MS stars such as  $\delta$  Scuti, SPB and  $\beta$  Cep variables. An extensive review on the effect of rotation on  $p$ -mode pulsation has been given by Goupil (2011).

## 9. Asteroseismic Modeling

Reliable calculation of stellar models is the main objective of the asteroseismic investigations. The pulsation properties are sensitive to small effects and it is necessary to use the best possible input physics when calculating a stellar model. It is necessary to include additional effects such as convective overshoot (Di Mauro et al. 2003a, 2003b), as well as diffusion and settling of helium and heavy elements (Vauclair et al. 1974). In most models the Coriolis and the centrifugal forces induced by rotation are generally neglected. When rotational is taken into account, it is usually done, only to first order where perturbation theory can be used. In case of solar-type stars, detailed classical models have been produced on several well observed targets viz.  $\alpha$  Cen (Guenther & Demarque 2000; Morel et al. 2000, Thévenin et al. 2002; Eggenberger et al. 2004);  $\eta$  Boo (Christensen-Dalsgaard et al. 1995; Di Mauro et al. 2004; Guenther 2004). A recent review on the problem and prospects of the modeling of the solar-like oscillators is presented by Di Mauro (2013).

A typical procedure of seismic modeling for the classical pulsators are as follow :

1. The pulsational modes are identified in terms of the quantum numbers ( $n, l, m$ ) that describe geometry of non-radial pulsations. The identification of these modes are the first step of the seismic modeling.
2. Photometric and/or spectroscopic time-series observations are used to

extract the frequencies, amplitudes and phases of the pulsations and to identify the modes whenever possible.

3. Evolutionary models which match the estimated physical parameters of the target stars are calculated. A pulsation model is used to calculate the expected frequencies which are then compared to the observed frequencies with known mode identifications. The physical parameters of the evolutionary model are adjusted until a best match with observed frequencies is obtained.
4. Once the best model is selected, the remaining frequencies without mode identification can be identified by the matching them with the predicted pulsation frequencies.

## 10. Pulsation Across the HR diagram

The location of the major classes of pulsating stars are illustrated in Fig. 1 and their pulsational characteristics are listed in Table 1. The shading in this figure describes the excitation and the type of modes; (a) horizontal shading indicates stochastically excited  $p$ -modes, (b) NW-SE shading (like Cepheids) indicates self-excited (predominately)  $p$ -modes and (c) SW-NE shading (like DAV) indicates self-excited  $g$ -modes.

One can broadly divide pulsating variables into three groups : The first group contains the large amplitude Cepheid, RR Lyrae and cool red variables which pulsate only in one or two radial modes. This group of stars follow a period-luminosity (PL) relation or a period-luminosity-colour (PLC) relation, making them useful as distance indicators (McNamara, 1995; Petersen & Christensen-Dalsgaard 1999;). The second group has low-amplitude oscillations in the mmag range exhibiting many radial and non-radial modes and includes the white dwarfs,  $\delta$  Scuti stars, roAp stars,  $\beta$  Cephei stars, SPB stars and the  $\gamma$  Dor stars. The third group has oscillations amplitude with amplitudes measured in  $\mu$ -mag and known as the solar-like oscillators.

Solar-like oscillations in main-sequence, sub-giants and giants are generally not visible from the ground except in a few cases. In the following subsections we give a brief introduction to the major classes of pulsating variables.

### 10.1 *Rapidly Oscillating Ap Stars*

The rapidly oscillating Ap (roAp) variables are sub-group of CP A-type cool ( $T_{eff} \sim 6400 - 8500K$ ) stars. These are hydrogen core burning MS stars of mass around  $2 M_{\odot}$  and exhibit strong dipole magnetic field of the order of a few kG. The peculiarity in these stars results from atomic diffusion, a physical process common in all the CP stars having extremely stable atmospheres. The roAp stars pulsate in period ranging from 5.7–23.6 min characterized as



Table 1 The names and basic pulsational characteristics of pulsating variables. In the table the term F is refers for fundamental and O is for overtones.

<i>Class</i>	<i>Other names</i>	<i>Mode Type</i>	<i>Period Ranges</i>	<i>Amplitudes (Light variation)</i>
Solar-like pulsator	main-sequence red giants, sub-giants	$p$ $p$	3 to 10 min few hrs to few days	<8 ppm few 10 ppm
$\gamma$ Dor	slowly pulsating F	$g$	0.3 to 3 d	< 50 mmag
$\delta$ Sct	SX Phe(Pop.II)	$p$	18 min to 8 h	< 0.3 mag
roAp	–	$p$	5.7 to 23.6 min	< 10 mmag
SPB	5 Per	$g$	0.5 to 5 d	< 50 mmag
$\beta$ Cep	$\beta$ CMa, $\zeta$ Oph 53 per	$p\&g$	2 to 8 h( $p$ ) few days( $g$ )	< 0.1 mag < 0.01 mag
pulsating Be	$\lambda$ Eri,SPBe	$p\&g$	0.1 to 5 d	< 20 mmag
pre-MS pulsator	pulsating T Tauri, Herbig Ae/Be, T Tauri	$p$ $p$ $g$	1 to 8 h 1 to 8 h 8 h to 5 d	< 5 mmag < 5 mmag < 5 mmag
$p$ -mode sdBV	EC14026, V361Hya	$p$	90 to 600 sec	< 0.3 mag
$g$ -mode sdBV	PG1716+426	$g$	0.5 to 3 h	< 0.01 mag
$p$ -mode sdOV		$p$	60 to 120 sec	< 0.2 mag
PNNV	ZZLep	$g$	5 h to 5 d	< 0.3 mag
DOV	, GW Vir	$g$	5 to 80 min	< 0.2 mag
DBV	V777Her	$g$	2 to 16 min	< 0.2 mag
DAV	ZZCeti	$g$	1 to 30 min	< 0.3 mag
RR Lyr	RRab RRc RRd	F FO F+FO	$\sim$ 0.5 d $\sim$ 0.3 d 0.3 to 0.5 d	< 1.5 mag < 0.5 mag < 0.2 mag
Type II Cepheid	W Vir BL Her	F F	0.8 to 35 d 1 to 8d	< 1 mag < 1 mag
RV Tauri	RVa,RVb	F?	30 to 150 d	< 3 mag
Type I Cepheid	Classical Cepheids s-Cepheid	F FO	1 to 135 d < 20d	< 2 mag < 0.1 mag
Mira	SRa, SRb SRc SRd	$l = 0$ $l = 0$ $l = 0$	> 80 d > 80d < 80d	< 8 mag < 1 mag < 1 mag

high-order ( $n > 20$ ), non-radial and low-degree  $p$ -modes (almost pure dipole  $l=1$ ). Typical amplitude of light variations lie in the range of 0.5-15 mmag and radial velocity variation amplitude are of about 0.05-5  $\text{kms}^{-1}$ . Most of roAp stars are multi-periodic, non-radial pulsators which makes them key objects for asteroseismology.

Currently about 60 roAp stars are known and majority of them belong to the Southern hemisphere. The observed pulsation properties of roAp stars

can be explained in terms of the oblique pulsator model (Kurtz 1982) in which the pulsation and magnetic axes are mutually aligned but tilted with respect to the rotation axis. This model was modified by Dziembowski & Goode (1996) and Bigot & Dziembowski (2002) who found that the pulsation axis is not in exact alignment with the magnetic axes. Fig. 19 and 22 show the sample light curves of two roAp stars and their corresponding amplitude spectrum are shown in Fig. 20 and 23. The excitation mechanism for the roAp stars is still an unresolved problem, although extensively debated over the years. In the H-R diagram they overlaps to the  $\delta$  Scuti star instability strip (see Fig. 1). It is thought that the strong magnetic field suppresses convection at the magnetic poles which drives the pulsation with high-radial overtones by the  $\kappa$  mechanism in the H-ionization zone.

Space missions such as *Kepler* has significantly improved our understanding of roAp stars and at the same time additional problems such as the unexpected appearance of low frequency modes have added (Balona et al 2011) and the possible detection of modes with different axes of pulsation (Kurtz et al. 2011).

Spectroscopy has now become an important tool for the detection of new roAp stars (Hatzes & Mkrtichian 2004; Elkin et al. 2005; Kochukhov et al. 2009). The advantages of spectroscopic observations over photometry is that the roAp stars have particularly high-radial velocity amplitudes in the lines of certain elements which are formed high in the atmosphere of the star. Several high-dispersion spectra taken over a few nights is sufficient to detect roAp oscillations which otherwise would have taken several weeks of photometry to detect. Such spectroscopic observations offer a unique opportunity to map the vertical structure of the pulsation modes (Ryabchikova et al. 2007) and for investigating the physics of propagating magneto-acoustic waves (Khomenko & Kochukhov 2009). The peculiar atmospheres of magnetic roAp stars offer the building of a 3-D model of a pulsating stellar atmosphere (Kochukhov 2004). The roAp stars have also been observed interferometrically. The first detailed interferometric study of the roAp star was applied on  $\alpha$  Cir for which allowed a radius  $R = 1.967 \pm 0.066 R_{\odot}$  was derived (Brunt et al. 2010).

## 10.2 $\delta$ Scuti Stars

The  $\delta$  Scuti stars are intermediate mass stars ( $\sim 1.4$  to  $3M_{\odot}$ ) of spectral types A2–F5. Their luminosity classes varies from III to V. Most of  $\delta$  Scuti stars belong to Population I but some of them show metallicities and space velocities typical to Population II. To date, several thousands of  $\delta$  Scuti stars have been found in our galaxy and these are among the most common type of pulsating star (Breger 1979).

Most of the  $\delta$ -Scuti stars are moderate or rapid rotators with surface velocities up to 100–200  $\text{kms}^{-1}$ . The  $\delta$  Sct stars pulsate in radial and/or

Table 2 Pulsation constant, Period and Period ratios for a typical  $\delta$  Scuti star.

Pulsation mode	Period	$P_i/P_{i-1}$	$P_i/P_F$	Q (days)
Fundamental, F	0.07861	-	1.000	0.0329
1st Overtone, 1H	0.05950	0.761	0.757	0.0251
2nd Overtone, 2H	0.04846	0.810	0.617	0.0203
3rd Overtone, 3H	0.04095	0.845	0.521	0.0172
4th Overtone, 4H	0.03533	0.862	0.449	-
5th Overtone, 5H	0.03109	0.879	0.396	-
6th Overtone, 6H	0.02774	0.882	0.353	-

non-radial low-order  $p$  modes with periods in the range 18 min to 8 hr and amplitudes from mmag up to tenths of a magnitude. The non-radial pulsations found photometrically are low-overtones ( $n = 0$  to 7) and low-degree ( $l \leq 3$ )  $p$ -modes. The radial pulsators mainly pulsate in the fundamental mode and its first few overtones. For a typical  $\delta$  Scuti star,  $T_{\text{eff}} = 7800$  K,  $M = 1.7 M_{\odot}$ ,  $L = 15 L_{\odot}$ ,  $Y = 0.28$  and  $Z = 0.02$  the pulsation constant, Q, and the ratio between periods is summarized in Table 2 (Breger 1979, Hareter et al. 2008).

Many  $\delta$  Scuti stars are multi-periodic variables therefore they are good candidates for asteroseismology. For example 79 and 29 frequencies are detected in FG Vir and 44 Tau, respectively (Breger et al. 2005). Fig. 10 shows the light curve and amplitude spectrum of a typical  $\delta$  Scuti star HD 98851 discovered from ARIES Nainital under the ‘‘Nainital-Cape Survey’’. The  $\delta$  Scuti stars are situated where the classical instability strip crosses the main sequence (see Fig. 1) hence the excitation mechanism of pulsation in  $\delta$  Scuti stars is the  $\kappa$ -mechanism, same as for other stars in the classical instability strip. The driving zone are *HI and He II* ionization zones which provides enough counterbalance to the damping in the underlying layers (Breger 2000).

The identification of the oscillation modes is a very complex task for  $\delta$  Scuti stars, since the asymptotic theory does not apply to the excited modes (low-order  $p$ -modes). Thus, at present, asteroseismology is able to put additional constraints on the internal structure of  $\delta$  Scuti stars. The P-L relations for  $\delta$  Scuti stars have been established in the V band (Petersen & Christensen-Dalsgaard, 1999; Pych et al. 2001; Templeton et al. 2002), V and R band (Garg et al. 2010) and V and I-Wesenheit-index (Majaess et al. 2011). Using these relations, one can determine the distance of these stars independently.

Thanks to the different space missions which provided asteroseismic data of  $\delta$  Scuti stars with very high precision. Matthews (2007) found 88 frequencies in the  $\delta$  Scuti star HD 209775 observed by MOST. The regular patterns

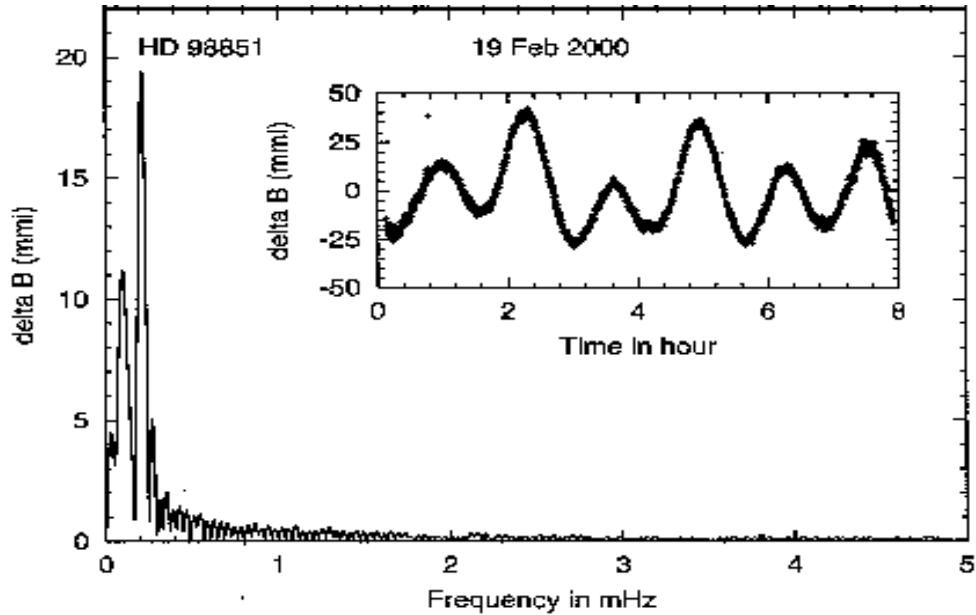


Figure 10 : Light curve and amplitude spectrum of HD 98851 observed from ARIES Nainital in 2000. Adopted from Joshi et al. (2003).

were also found in the oscillation spectra of  $\delta$  Scuti stars observed by *CoRoT* and *Kepler* (García et al. 2013 ; Mantegazza et al. 2012).

There are two well-defined sub-groups of  $\delta$  Scuti stars : (1) High-amplitude  $\delta$  Scuti stars (HADS) which are first classified as AI Velorum stars. These stars pulsate in the fundamental or first overtone modes with V-amplitude  $\geq 0.3$ -mag and follow the P-L relation. Hence they have been used to estimate the distance of the LMC and to star clusters; (2) SX Phoenicies (SX Phe) are  $\delta$  Scuti stars of Population II, with shorter periods and lower amplitudes. They have been found in globular clusters and are known as Blue Stragglers. From an evolutionary point of view they are unusual and understood resulted from merged binary stars (Mateo et al. 1990).

### 10.3 $\gamma$ Dor Stars

Balona et al. (1994) discovered a new group of Pop I stars known as  $\gamma$  Dor which are the main-sequence stars that partly overlap the cool edge of the  $\delta$  Scuti instability strip. About 50 confirmed members of this class are known to the date and more than 100 additional candidates are being studied observationally (Henry et al. 2005; De Cat et al. 2006). The  $\gamma$  Dor stars are early-type-F stars that have masses between  $1.5$  and  $1.8M_{\odot}$  and

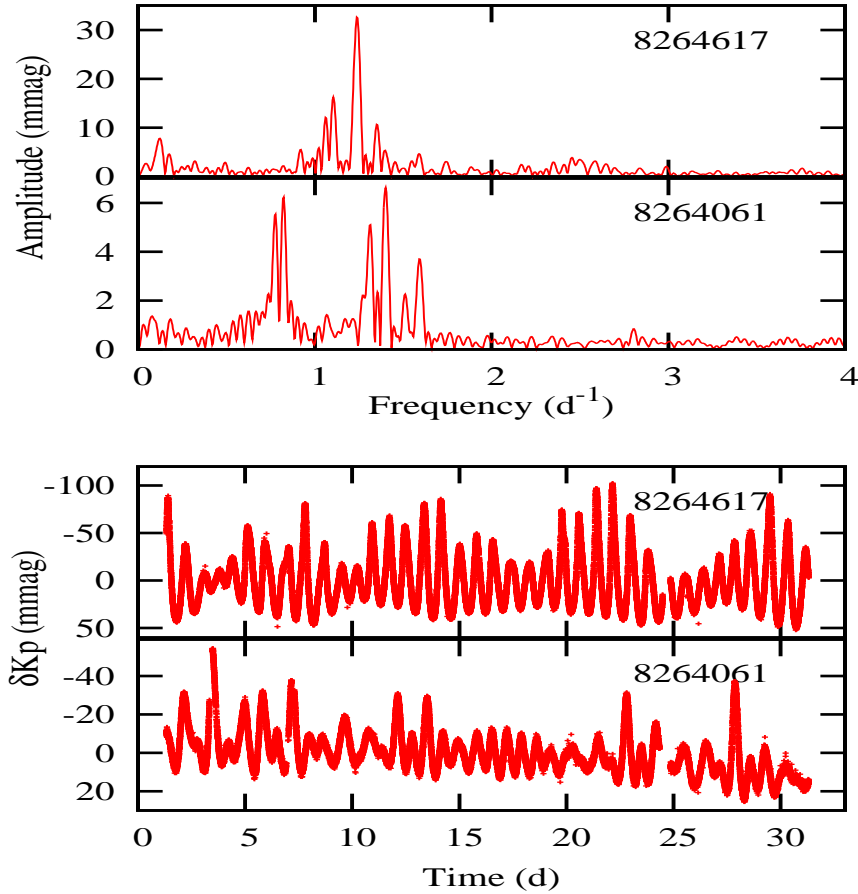


Figure 11 : Light curve (bottom) and periodograms (top) of two  $\gamma$  Dor stars KIC8264617 and KIC8264061 in the field of open star cluster NGC6866. Adopted from Balona et al. (2013).

pulsate in multiple non-radial,  $g$ -modes with periods ranging from 0.3 to 3.0 d. The high-order  $g$ -modes are driven by a modulation of radiative flux from the interior of the star due to the convection zone, a mechanism known as convective blocking (Guzik et al. 2000)

Stars that exhibit both  $p$ -modes and  $g$ -modes are very important for the asteroseismic study because they pulsate with many simultaneous frequencies and can probe both the surface and core region of the stars. There is considerable overlap between the  $\delta$  Sct and  $\gamma$  Dor instability strips where both the high-frequencies  $\delta$  Sct and the low-frequencies  $\gamma$  Dor stars are found. These stars are known as hybrid stars (Grigahcène et al. 2010; Antoci et

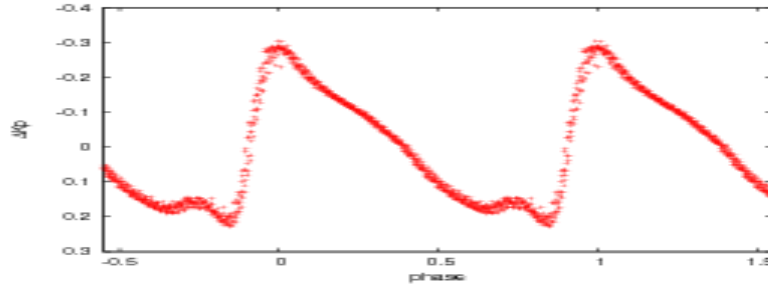


Figure 12 : Phase light curve plot of RR Lyr at maximum and minimum amplitude. Adopted from Szabó (2010).

al. 2011) and first discovered in the A9/F0V star HD 209295 (Handler et al. 2002).

#### 10.4 RR Lyrae Stars

The RR Lyrae are evolved low-mass ( $M \leq 7M_{\odot}$ ) stars of spectral type A2-F6 on the horizontal branch (core He burning) with a low content of heavy elements and are commonly found in globular clusters and in the Magellanic Clouds. About 90 percent RR Lyrae pulsates radially either in fundamental or first overtone modes with period 0.2 to 0.5 d having amplitude between 0.2 to 1.5 mag in V band. In the H-R diagram, they are located just below the Cepheids in the instability strip. Due to their mono-periodicity, RR Lyrae are not suitable for the seismic study but they follow a period-luminosity-color relation, hence can be considered standard candles for distance measurements and galactic evolution (Kolenberg et al. 2010).

In one member of the class, Blazhko (1907) discovered that the maximum amplitude varied cyclically with a period of 40.8 d i.e. amplitude and phase modulation (Kolenberg 2008). Using *Kepler* data, Szabó et al. (2010) found Blazhko effect in three RR Lyrae stars which showed period doubling in certain phases of the Blazhko cycle, with slight variations in the maximum amplitude between alternating pulsation cycles. The two competing theoretical explanations for the Blazhko effect are : (1) caused by the excitation of a non-radial oscillation mode of low-degree apart from the main radial mode, through non-linear resonant mode coupling. In this model the Blazhko period is interpreted as the beat period between the radial fundamental and a non-radial mode (Dziembowski & Cassisi 1999); (2) caused by a magnetic field that influences the oscillations similar to the oblique pulsator model for the roAp stars. In this case the Blazhko period is interpreted as the rotation period of the star (Takata & Shibahashi 1995).

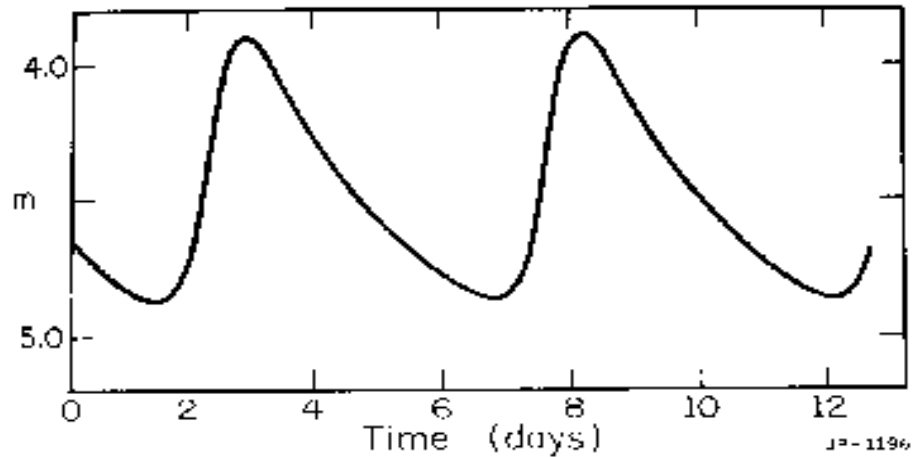


Figure 13 : Typical light curve of a Cepheid.

### 10.5 Cepheids

Cepheids are population I yellow super-giants of spectral class F6 - K2. These are very luminous stars with luminosity 500 to 300,000 times more than the Sun, pulsate with periods from 1 to 135 days and light variations from 0.1 to 2 mag. The light curve of one of typical  $\delta$  Cephei is shown in Fig. 13. By measuring the oscillation period of a Cepheid and using the period-luminosity relation, one can derive the absolute magnitude, hence distance of the star. For this reason, Cepheids are also called distance indicators. While stellar parallax can only be used to measure distances to stars within hundreds of parsecs but Cepheids can be used to measure the larger distances of the galaxies where they belong. Today we recognize the following stars as distinct classes of Cepheids :

#### 10.5.1 Classical Cepheids or Type I Cepheids

These are massive ( $M \sim 5-15M_{\odot}$ ) young bright giants or super-giants of spectral types F or G and are found exclusively in the disk population of galaxies. The periods of this class lie in the range  $1 < P < 135$  d, with amplitudes of 0.5-2 mag. Cepheids are core He burning stars and cross the instability strip up to three times.

#### 10.5.2 *W Vir* stars

These are evolved F6-K2 Population II giants with periods in the range  $0.8 < P < 35$  d and amplitudes of 0.3-1.2 mag. Their light curves generally

resemble those of the classical Cepheids, particularly if they have a period of 3–10 d. Typically, they have lower masses than classical Cepheids are about 1.5 mag fainter than classical Cepheids of the same period and obey a different P-L relation.

### 10.5.3 *BL Her stars*

These Cepheids have periods less than about 8 days and mostly are metal deficient and thought to be post-horizontal branch stars. They have a characteristic bump on the declining branch of the light curve.

### 10.5.4 *RV Tauri stars*

The RV Tauri are characterized by alternating deep and shallow minima in their light curves with periods 30–150 d measured between successive deep minima. These stars have spectral types F–G at minimum and G–K at maximum. RV Tauris are probably low-mass stars in transition from the asymptotic giant branch to white dwarfs.

## 10.6 *Slowly Pulsating B Stars*

The Slowly Pulsating B Stars (SPBs) are situated along the MS indicating that nuclear core hydrogen burning is still ongoing. SPBs are massive hot stars with spectral types ranging between B2 and B9, corresponding to effective temperatures of 12000K up to 18000 K. Their masses lie in the range between  $3M_{\odot}$  to  $7M_{\odot}$ . All the known members of this class are slow rotators in the sense that the observed projected rotational velocities are much smaller than the break-up velocities of such stars. The SPB stars are mid-to-late B-type stars oscillating in high-order  $g$ -modes with periods from 0.3 to 3 days similar to the 53 Per stars. These oscillations are driven by the  $\kappa$ -mechanism operating in the iron ionization zone located at  $T_{eff} \sim 200000$  K (Gautschy & Saio 1993). Since most SPB stars are multi-periodic, hence the observed variations have long beat periods and are generally complex.

## 10.7 *$\beta$ Cephei Stars*

The  $\beta$  Cep stars have been known as a group of young Population I near MS pulsating stars for more than a century. They have masses between 8 and 18  $M_{\odot}$  and oscillate in low-order non-radial  $p$ - and  $g$ -modes with periods between 2 and 8 h with amplitudes less than 0.3-mag in V band (Moskalik 1995). More than 100 members of this group are known and the class contains dwarfs up to giants (Stankov & Handler 2005). Most of the  $\beta$  Cep stars show multi-periodic light and line profile variations (Pamyatnykh 1999), hence considered as excellent objects for the asteroseismology (Balona et al. 2011).



## 10.8 *Mira Variables*

Miras represent the advanced evolutionary stages of low and intermediate mass stars such as Sun. These are class of pulsating variables characterized by pulsation periods between 10 and 100 days with amplitudes greater than 2.5-mag in V-band. These are cool red giant and are found in the high-luminosity portion of the asymptotic giant branch (AGB) in the H-R diagram (Tabur et al. 2009). There is some dispute whether they pulsate primarily in their fundamental or first overtone (Wood 1995), and there is evidence that some Miras switch between different modes on time scales of decades (Bedding et al. 1998).

## 11. Sub-dwarf B Variable Stars

The Sub-dwarf B (sdB) stars are core-helium burning stars of  $\sim 0.5M_{\odot}$  with a very thin surface layer of hydrogen. With effective temperatures  $25000 \leq T_{\text{eff}}/K \leq 35000$ , the atmospheres of these stars are entirely radiative. On the HR diagram, the sdB stars are found between the upper main sequence and the white dwarf sequence. Pulsations in sdB were first observed in such stars by Kilkenney et al. (1997) characterized as low-degree ( $l$ ), non-radial multi-periodic  $p$ -mode pulsators with period  $65\text{-sec} \leq P \leq 500\text{-sec}$ , and amplitudes ranging from 1 mmag up to 0.3 mag. The driving arises from the  $\kappa$ -mechanism operated by opacity from the iron-group elements. Three types of pulsating sub-dwarf star are known: long-period sub-dwarf B (sdB) stars (PG1716 or V1093 Herculis stars) that oscillate in high-overtone,  $g$ -modes with periods from 30 to 180 minutes, short-period sdB stars pulsating in low-overtone,  $p$ - and  $g$ -modes with periods from 90 to 600 sec (EC14026 or V361 Hydrae stars), and the oscillating sub-dwarf O (sdO) stars are low-overtone  $p$ -mode pulsator with periods from 60 to 120 sec. Fig. 14 shows a portion of the light curve obtained with ULTRACAM a high-speed 3-channel CCD camera mounted on the 4.2 m William Herschel telescope. At ARIES we are developing a similar three channel fast CCD photometer for the 3.6-m telescope (see Sec. 15).

### 11.1 *Solar-like Oscillations*

The well known solar-like oscillator is of course the Sun and its frequency spectrum is shown in Fig. 3 where one can see hundreds of peaks centered at 3 mHz ( $P=5$  min). The solar-like oscillation can be expected in low-mass main-sequence stars, sub-giants, stars on the red-giant branch (RGB) horizontal branch and asymptotic-giant branch (Christensen-Dalsgaard & Frandsen 1983; Houdek et al. 1999, Dziembowski et al. 2001). The oscillation periods in these stars are expected to be in the range from the typical 5-min (MS stars), as in the Sun, up to about a few days in sub-giant and

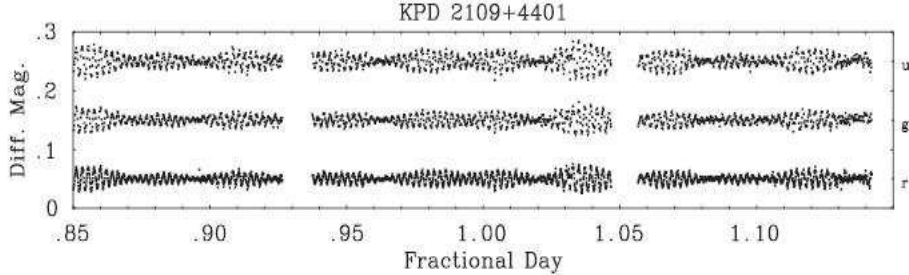


Figure 14 : Partial ultracam light curves for sdBVs KPD 2109+4401. Adopted from Jeffery et al. (2004).

giant stars. According to theoretical estimations (Kjeldsen & Bedding 1995) the expected luminosity variations are of the order of a few mmag in giant stars while in MS and sub-giant stars are of the order of ppm which is below the detection limit for ground-based photometric observations. The radial velocity amplitudes are expected to be atmost 50-60 m/sec in K giants, 1-2 m/sec in F and G sub-giants and even smaller in main-sequence solar-type stars.

The observed modes of solar-like oscillators are typically high-order non-radial, acoustic  $p$ -modes. However a distant observer can usually not resolve the stellar surface and can only measure the joint effect of the pulsations in light and radial velocity. As a consequence, the effects of high-spherical degree oscillations average out in disk-integrated measurements (Dziembowski 1977) and due to this only modes of low-angular degree ( $l$ ) can be observed. A revolution in the detection of solar-like oscillation took place photometric observations after the launch of *MOST*, *CoRoT* and *Kepler* space missions. The *Kepler* has yielded clear evidence of solar-like oscillations in more than 500 solar-type stars (Chaplin et al. 2011).

The simplest analysis of asteroseismic data of the solar-like oscillators is based on the overall properties of the oscillations. In the periodogram, solar-like oscillations are easily identified because of the localized comb-like structure where amplitudes decrease sharply from a central maximum. Fig. 15 shows an example of comb-like structure generally found in solar-like oscillators. structure. The frequency of maximum amplitude ( $\nu_{\max}$ ) and large separation ( $\Delta\nu$ ) between successive overtones of the same degree depends on the mean density of the star (Ulrich 1986; Kjeldsen & Bedding 1995) and expressed as :

$$\frac{\nu_{\max}}{\nu_{\max\odot}} \approx \frac{M/M_{\odot}}{(R/R_{\odot})^2 \sqrt{T_{\text{eff}}/T_{\text{eff}\odot}}}, \quad (12)$$

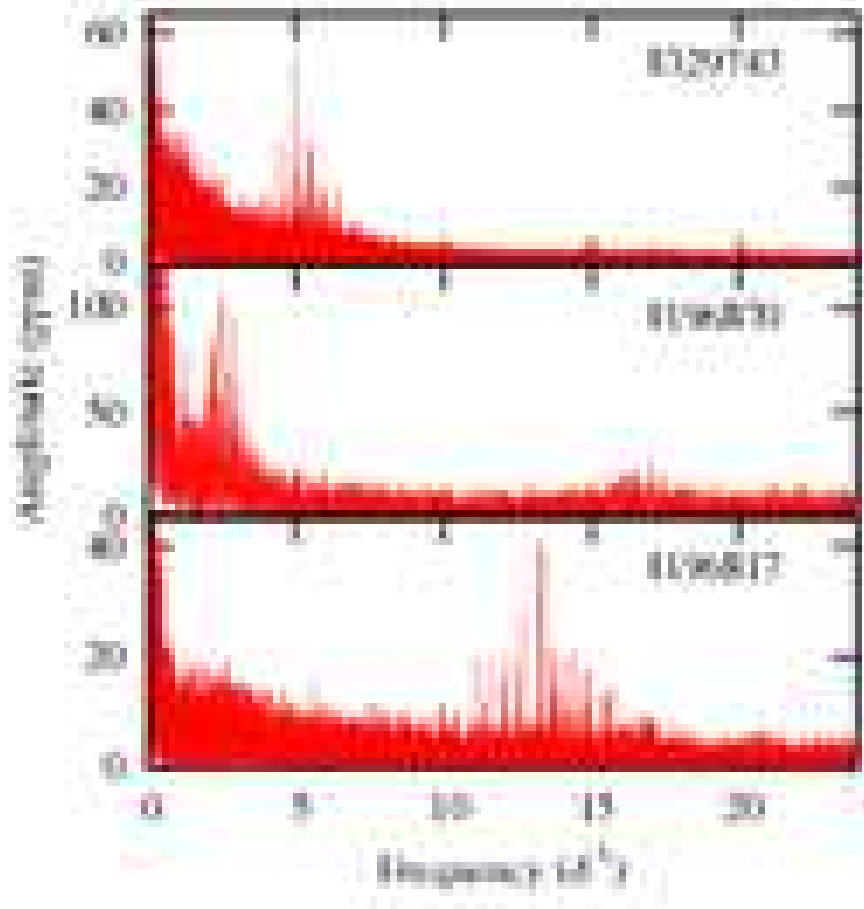


Figure 15 : Periodograms of three solar-like oscillators the field of open star cluster NGC 6866 observe by *Kepler*. Adopted from Balona et al. (2013).

where  $T_{\text{eff},\odot} = 5777$  K,  $\nu_{\text{max}\odot} = 3120 \mu\text{Hz}$  (Kallinger et al. 2010),  $M/M_{\odot}$ ,  $R/R_{\odot}$  and  $T_{\text{eff}}/T_{\text{eff}\odot}$  is the stellar mass, radius and effective temperature relative to the Sun.

$$\frac{\Delta\nu}{\Delta\nu_{\odot}} \approx \frac{(M/M_{\odot})^{1/2}}{(R/R_{\odot})^{-3/2}} \quad (13)$$

The above scaling relations can be easily expressed in the terms of stellar radius  $R$  and mass  $M$  as function of  $\delta\nu$ ,  $\nu_{\text{max}}$  and effective temperature  $T_{\text{eff}}$ :

$$\frac{R}{R_{\odot}} = \left( \frac{\nu_{\max}}{\nu_{\max,\odot}} \right) \left( \frac{\delta\nu}{\delta\nu_{\odot}} \right)^{-2} \left( \frac{T_{\text{eff}}}{T_{\text{eff},\odot}} \right)^{1/2} \quad (14)$$

$$\frac{M}{M_{\odot}} = \left( \frac{\nu_{\max}}{\nu_{\max,\odot}} \right)^3 \left( \frac{\delta\nu}{\delta\nu_{\odot}} \right)^{-4} \left( \frac{T_{\text{eff}}}{T_{\text{eff},\odot}} \right)^{3/2} \quad (15)$$

Thus, provided that  $T_{\text{eff}}$  is known, both radius and mass of solar like oscillations can be easily derive from the frequency spectrum. This technique has been applied to huge samples of MS, sub-giant and red-giant stars (Bedding & Kjeldsen 2003; Chaplin 2011a,b; Huber 2011; Stello et al. 2008; White et al. 2011; Miglio et al. 2012; Hekker et al. 2013). Efforts have recently been taken to test the accuracy of the scaling relations and asteroseismically inferred properties. The reliability of the mass and radius estimates from these relations depends on the validity of the scaling laws themselves. For a comprehensive review on solar-like oscillations see Chaplin & Miglio (2013) and references therein.

### 11.2 Planetary Nebula Nuclei Variables

The Planetary nebula nuclei variables(PNNV) are pre-white dwarf stars situated at the center of planetary nebula. These are multi-periodic variable pulsate with period 10–35 min with amplitudes of around 0.1 mag.

### 11.3 White Dwarfs

White dwarfs are the final evolutionary stage of about 98% of stars. A fraction of them are  $g$ -mode pulsators with hydrogen atmospheres and are located in a narrow range of effective temperature  $10500 < T_{\text{eff}} < 12300\text{K}$  (Winget & Kepler 2008; Althaus et al. 2010). In fact other than the Sun white dwarfs represent the stars in which the largest number of oscillation frequencies have been detected. When the white dwarfs evolve and pass through the instability strip they become pulsators and known as the DAV (ZZ Ceti), DBV (V777 Her) and DOV (GWVir) (D = white dwarf; V = pulsating variable; and O(hot), B(warm) and A(cool) refer for spectral type. The ZZ Ceti (or DAV) stars are the most numerous class of degenerate white dwarfs, with  $\sim 160$  members known to date (Castanheira et al. 2013). Their photometric variations are characterized as non-radial  $g$ -mode pulsations with low-harmonic degree ( $l \leq 2$ ) of periods range 70 to 2000 sec with amplitude variations up to 0.3 mag.

The driving mechanism thought to excite the pulsation near the blue edge of the instability strip is the  $\kappa - \gamma$  mechanism acting on the hydrogen partial ionization zone (Winget et al. 1982). Fig. 16 shows a typical light curve of a DAV white dwarf HL Tau 76 observed from ARIES Nainital under a multi-site campaign.

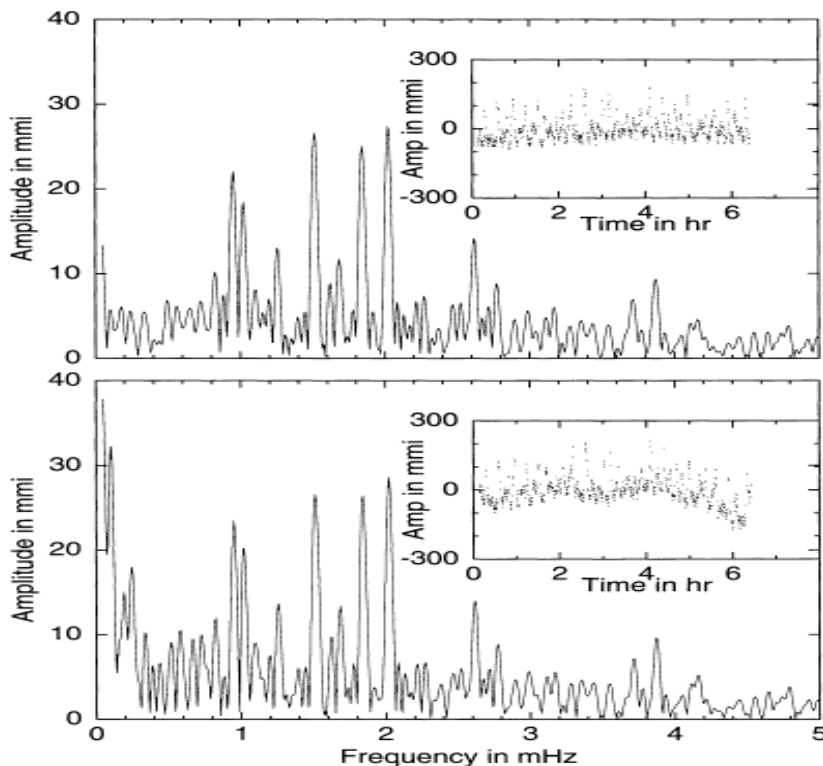


Figure 16 Light curve of a DAV (ZZ Ceti) white dwarf observed from *ARIES* in 1999. Adopted from Ashoka et al. (2001).

White dwarfs asteroseismology acts the comparison between the observed pulsation periods and the periods computed for appropriate theoretical models to place the observational constraints on their stellar mass, the thickness of the outer envelopes, the core chemical composition, magnetic fields, rotation rates and crystallization process (Montgomery & Winget 1999; Metcalfe et al. 2004; Corsico et al. 2005; Kanaan et al. 2005). The rate of period change can be employed to measure their cooling rate (Kepler et al. 2005). Many attempts have been undertaken to derive the internal rotational profiles by using the observed splitting and adopting forward calculations. The inversion techniques for white dwarfs have been presented in several works by Kawaler et al. (1999) and Vauclair et al. (2002).

## 12. Asteroseismology of Clusters

Stars in clusters are believed to formed from the same cloud of gas roughly at the same time, hence the cluster members are therefore expected to have

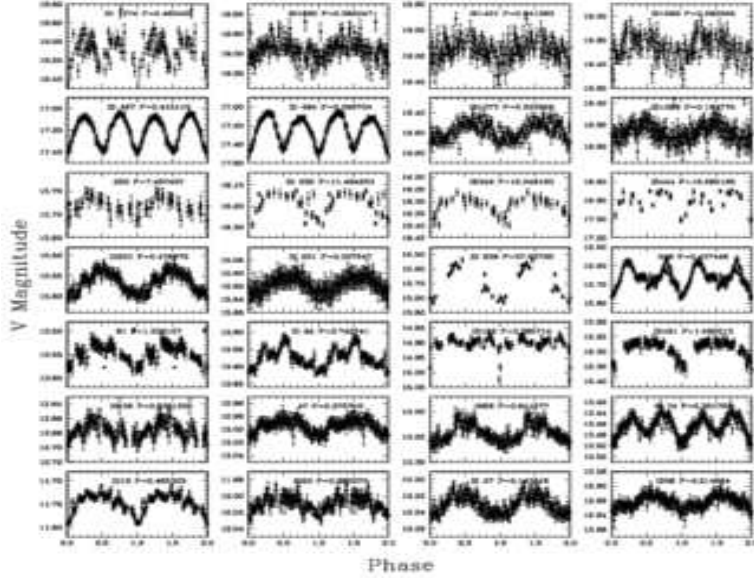


Figure 17 : V-band phased light curve for the 28 variable stars identified in this study. Adopted from Joshi et al. (2012a)

common properties. Asteroseismology of clusters is a potentially powerful tool to test aspects of stellar evolution that cannot be addressed otherwise. The advantage of cluster asteroseismology is that the seismic data do not suffer from uncertainties in distance or extinction and reddening and for this reason, ensemble asteroseismology is suitable for cluster stars (Stello et al. 2010, 2011a,b; Miglio et al. 2012; Chaplin et al. 2014; Wu et al. 2014a).

To bring a new dimension to ensemble asteroseismology one need high duty observations cycle and with a long time base of at least half a year to detect rotational splitting of the pulsation modes of numerous cluster stars, including the slowest rotators. Prior to *Kepler* survey many attempts were undertaken to detect solar-like oscillations in open and globular clusters (Gilliland et al. 1993; Stello et al. 2007a,b; Stello & Gilliland 2009). Stello et al. (2010) obtained the clear evidence of the detections of solar-like oscillations in red giants of open cluster NGC6819 and were able to measured the large frequency separation ( $\Delta\nu$ ), and the frequency of maximum oscillation power ( $\nu_{max}$ ).

Distance is a fundamental parameter in astrophysics which can be derived using the data from Hipparcos satellite (Perryman & ESA 1997), binary systems (Brogaard et al. 2011), isochrone fitting (Bedin et al. 2008; Hole et al. 2009; Wu et al. 2014a), red-clump stars as standard candles (Garnavich et al. 1994; Gao & Chen 2012), the P-L relation of pulsating stars (Soszynski

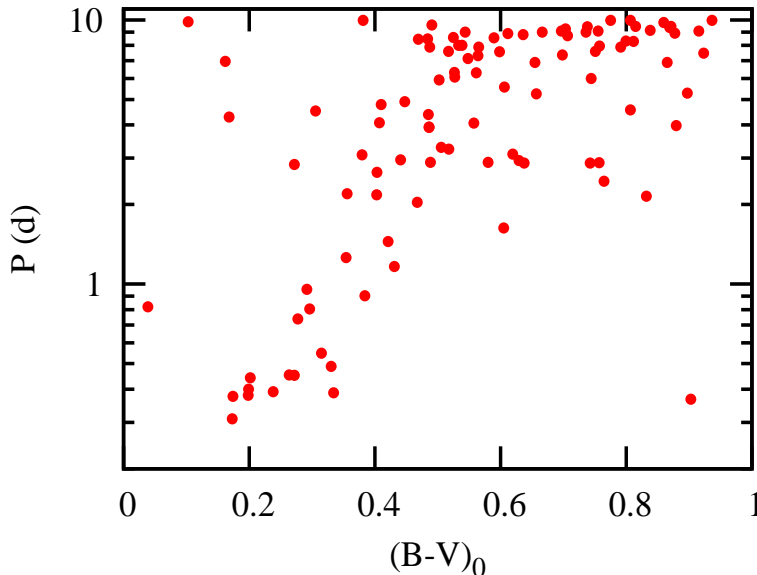


Figure 18 : Rotation period  $P$  (in d) as a function of  $(B - V)_0$  for main-sequence stars in the field. Adopted from Balona et al. (2013)

et al. 2010). Wu et al. (2014b) derived a new relation for distance of two clusters NGC 6791 and NGC 6819 by measuring the global oscillation parameters  $\Delta\nu$  and  $\nu_{max}$ . Stello et al. (2010) performed an asteroseismic analysis based on the first month of data from the *Kepler* Mission to infer the cluster membership for a small sample of red giant stars in NGC 6819. The authors demonstrated that cluster membership determined from seismology show more advantages over other methods.

In order to investigate the occurrence of pulsation in A- and F-type stars in different galactic environments, at ARIES we initiated a survey to search for the photometric variability in the young and intermediate age open star clusters. We selected sample of clusters having different age (young to intermediate of age range 10 to 100 Myrs). The preliminary results of the survey resulted 18 new variables in an open star cluster NGC6866 (Joshi et al. 2012a). The V-band phased light curves of 28 variables are shown in Fig. 17.

This cluster belongs to the *Kepler* field, therefore an analysis of stars in the field of the open cluster NGC 6866 was performed time-series photometry from the *Kepler* data. We identified 31  $\delta$  Scutis, 8  $\gamma$  Dor pulsating variables and 23 red giants with solar-like oscillations. There are 4 eclipsing binaries and 106 stars showing rotational modulation with indication of star-spots. We attempted to identify cluster members using their proper motions but

found very poor discrimination between members and non-members (Balona et al. 2013).

The rotation periods of the MS stars are correlated with colour, so that a period–age–mass relation can be derived from open clusters and applied to stars of unknown ages. We noticed that the correlation applies not only to cool stars but extends up-to A-type stars in the cluster which is shown in Fig. 18. We conclude that either the role of convection in A-type stars is not fully appreciated or that something other than convection is at the root of the rotation period-mass-age relationship (Balona et al. 2013).

### 13. ARIES Contribution towards the Asteroseismology

ARIES is contributing significantly in the area of asteroseismology since last two decades. In the following sub-sections we high-light the programmes where we participated for the asteroseismic study of pulsating variables.

#### 13.1 *The Nainital-Cape Survey*

Aiming to search for the new roAp stars in the northern hemisphere a survey “The Nainital-Cape Survey” is being carried out at ARIES since year 1999. The high-speed/fast photometric technique was adopted for the survey. Each star was observed through a Johnson B filter with continuous 10-sec integration. The observations were acquired in a single-channel with occasional interruptions to measure the sky background, depending on the phase and position of the moon. To minimize the effects of seeing fluctuations and tracking errors an aperture of 30'' was selected. Each target was observed continuously for 1 to 3 hours a sufficient time to reveal the roAp like oscillations. The results obtained from this survey are described by Martinez et al. (2001); Girish et al. (2001); Joshi et al. (2003; 2006; 2009; 2012b).

Based on the Strömgren colours we searched for the rapid oscillations in HD 12098 on the night of 21 November 1999 (HJD 2451504). We were rewarded with the discovery of 7.6-min oscillation which was confirmed on the nights of HJD 2451505, 2451534 and 2451535. Fig. 19 shows the light curve obtained on night of HJD 2451535 and Fig. 20 shows the amplitude spectra of the light curves obtained during the follow-up observations. The analysis of data of individual night clearly shows the modulation in the amplitude of oscillation.

A multi-site campaign was organized on HD 12098 in Oct/Nov 2002 aiming to search for additional frequencies and derive the basic physical parameters. The campaign involved a total of ten observatories and of 394 hours of useful data extending over 28 nights with 45% duty cycle were obtained. The equal separation of the frequencies seen in the multi-site data gives a rotation period of  $\Omega = 5.41 \pm 0.05$  day for HD 12098 which is very close to the 5.5 days rotation period predicted by Girish et al. (2001).



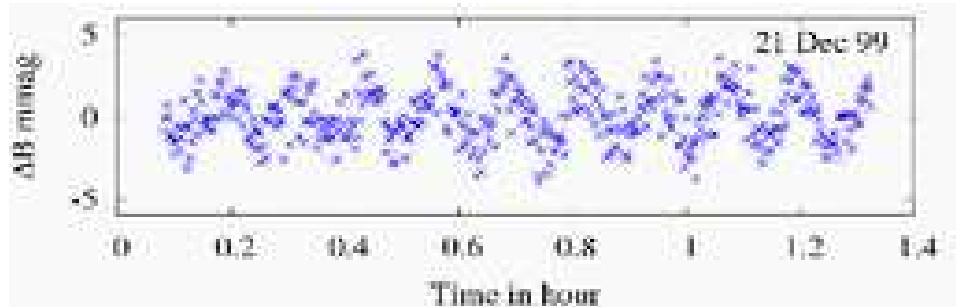


Figure 19 : Light curve of HD12098 observed on the night of 21 December 1999. Each dot represents a 10-s integration. Adopted from Girish et al. (2001).

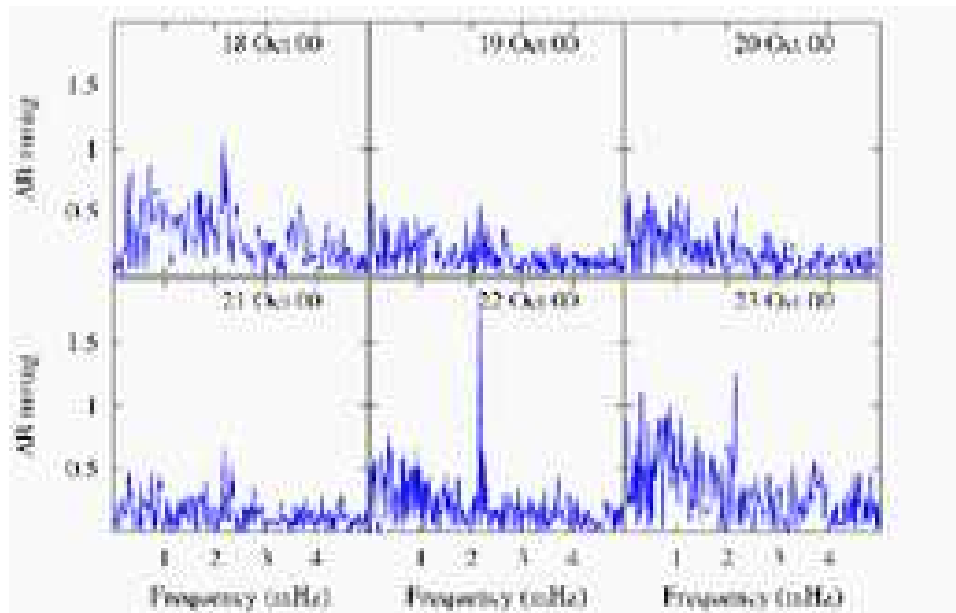


Figure 20 : Amplitude spectrum of the time-series of HD 12098 obtained on different nights. Adopted from Girish et al. (2001).

### 13.2 WET Campaign on pulsating sdBV

Astronomers at various observatories in India are involved in the observation of variable phenomena in astronomical objects where continuous observations are required. The observational coverage from the Asian longitudes

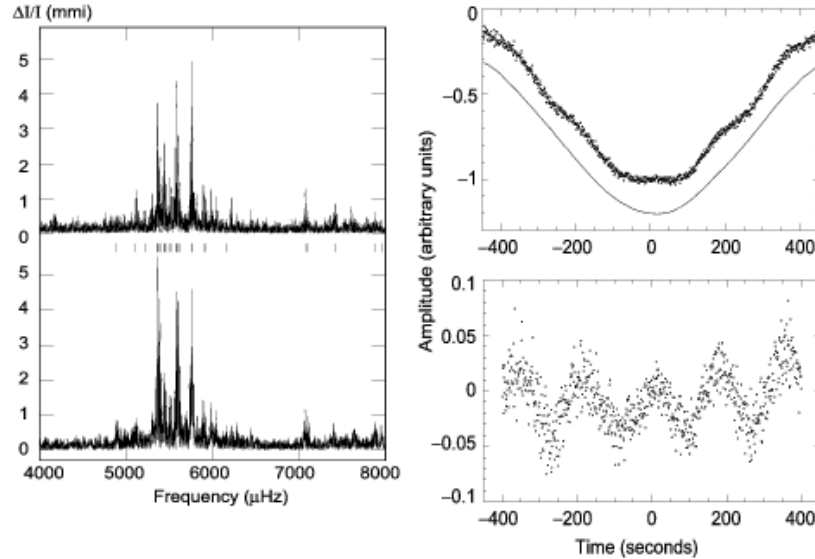


Figure 21 : The figure on the left side shows the frequency spectrum of PG1336-018 obtained during two halves of the WET run in April 1999. The figure on the right side shows the presence of pulsations during the eclipse after removing the eclipse profile with best fit. Adopted from Kilkenney et al. (2003).

are very important to fill critical gaps in the data sets. In order to take the advantage of the geographical location of India, we first joined the WET organization in November 1988 to observe V471 Tau and since then we have participated in seven campaigns. ARIES participated in the multi-site campaign organized for PG 1336-018 (NY Vir) which is a close eclipsing binary with a binary period of 2.4 hr (0.101d) and one of the components of this binary system is a pulsating B sub-dwarf (sdBV).

PG 1336-018 was observed in April 1999 under the WET campaign and 172 hours of observation with 47% coverage was obtained. The main aim of the campaign was to look for pulsations during eclipse and if well resolved, mode identification would be possible depending on the gradual decrease/increase in amplitude of the frequencies during ingress/egress. More than 28 frequencies were detected with 20 frequencies were identified in the frequency range of 4000 to 8000  $\mu\text{Hz}$  down to an amplitude of 0.003 modulation intensity level (Kilkenney et al. 2003). The sensitivity limits of the WET enabled the detection of very low-amplitude pulsations even during eclipse. Fig. 21 shows the light curve and frequency spectrum obtained during the campaign. The inclination of the system is estimated to be 81 degrees, and therefore even during primary eclipse, pulsations were expected.

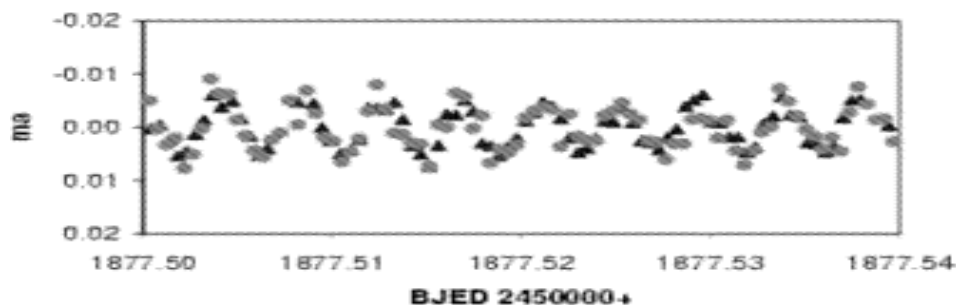


Figure 22 : A section of 1-hr light curve of HR 1217. Adopted from Kurtz et al. (2005).

One important result obtained from the WET campaign was that during the eclipse, pulsations were indeed observed, however due to insufficient coverage of eclipses during the campaign the pulsational modes could not be identified.

### 13.3 WET Campaign on *roAp* Star HR 1217

The birth of the asteroseismology at ARIES began with the “Nainital-Cape Survey” project for the quest of new *roAp* stars in the Northern hemisphere. ARIES participated in the WET campaign for HR 1217, one of the best-studied *roAp* star which exhibited six oscillation frequencies each of these showing rotational modulation (Kurtz et al. 1989). The result showed that 5 adjacent frequencies groups in the previous data could be explained by splitting main frequency and the 6<sup>th</sup> frequency is 3/4 of the splitting frequency was unexplained. To explain it, a whole earth campaign was organized and data was collected over 35 d with a 34% duty cycle in November - December 2000 when a total of 342 hr data through Johnson *B* data with 10-s time resolution was obtained. The precision of the derived amplitudes is 14- $\mu$ mag, makes the highest precision ground-based photometric studies ever undertaken. The multi-site data clearly shows amplitude modulation for some modes between 1986 and 2000.

Fig. 22 shows a section of the light curve of HR 1217 observed under this campaign and Fig. 23 shows a schematic amplitude spectrum of the determined frequency. An additional peak was detected at 2788.95  $\mu$ Hz with amplitude 0.1 mmag (Kurtz et al. 2002). The amplitudes of various modes change with time and this could be the reason for the non-detection of the new frequency in the 1986 dataset and its detection in 2000 can be confirmed only with future observations.

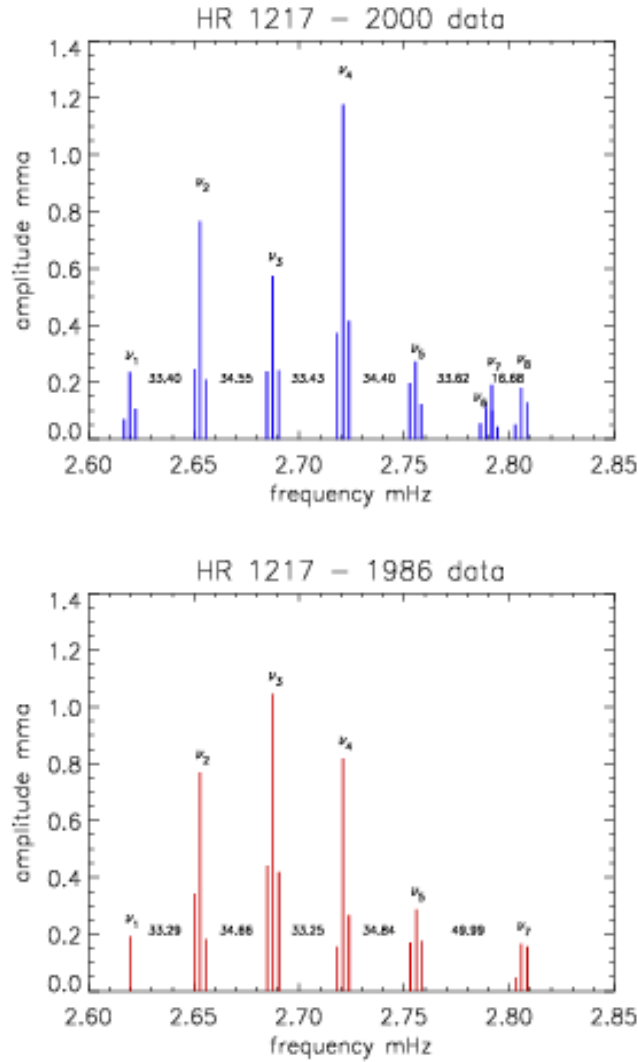


Figure 23 : The difference in the Fourier spectra of the WET data set (top) and the 1986 dataset (bottom). Adopted from Kurtz et al. (2002).

#### 13.4 *WET Campaign on Pulsating White Dwarfs*

ARIES participated in the WET campaigns organized for DA (ZZ Ceti) and DB white dwarfs. To check the stability of the pulsation periods an extensive multi-site data of ZZ Ceti was carried out. The analysis of these observations concluded that the characteristic stability time-scale for the pulsation period is more than 1.2 Gyr comparable to the theoretical cooling time-scale typical for this star (Mukadam et al. 2003).

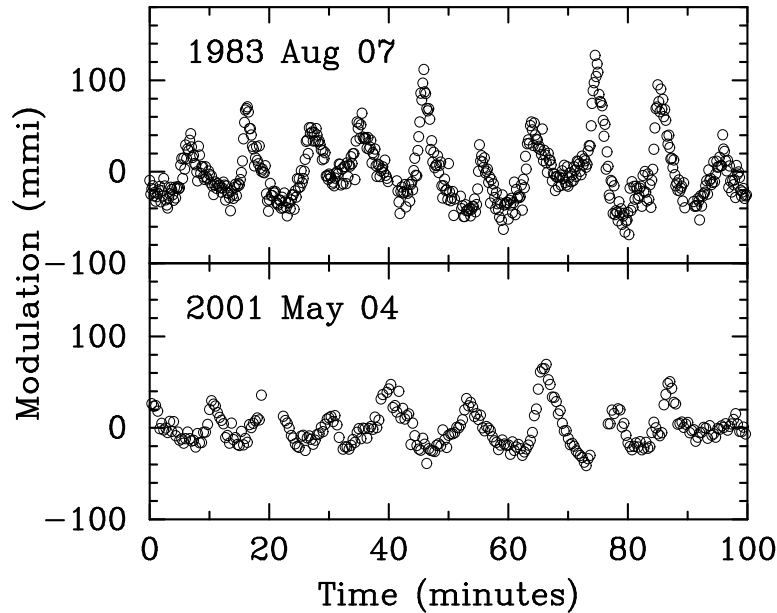


Figure 24 : Upper panel: the discovery light curve of KUV05134+2605. Lower panel: section of one of the light curve acquired during the WET run. Note the change in the pulsational time scales and amplitudes. Adopted from Handler (2003).

To study the temporal behavior of the pulsational amplitudes and frequencies of DBV pulsating the time-series photometry of KUV05134+2605 were carried out under the WET campaign. Fig. 24 shows a part of the light curve of KUV05134+2605 observed during this campaign. For the comparison, the previously obtained light curve is also shown in the upper panel. The beating of multiple pulsation modes cannot explain simply and the amplitude variability could be intrinsic (Handler 2003).

## 14. Future Prospects

We have seen that many efforts from the ground and spaced based instruments are being taken to obtained the high-precision data to improve the stellar models. However, there is a continuous need to improve the observational situation and strong prospects for the stellar structure and evolution. To reduce the gaps in the data, ground based observations can be carried out in a co-ordinated fashion by involving two or more observatories. This is one of the motivation for the development of the Stellar Observations Network Group (SONG)(Grundahl et al. 2009, 2011) which is consist of 8 nodes with a suitable geographical distribution in the Northern and Southern hemi-

sphere. Each node has a robotic telescope of diameter 1-m equipped with a high-resolution spectrograph (resolution of  $10^5$ ) capable of reaching a RV precision of  $1 \text{ ms}^{-1}$  for stars down to magnitude  $V = 6$  for Doppler velocity observations and high-speed camera for photometry of crowded fields. The first node of SONG network is commissioning in Tenerife, a Chinese node is under construction, and additional nodes are expected to be added in the near future.

The success of the MOST satellite gave the idea of building small and relatively inexpensive satellites (also called nano-satellites) the first space mission dedicated to the observations of the stellar oscillations (Walker et al. 2003). The BRiGht Target Explorer mission (BRITE) is a constellation of Austrian-Polish-Canadian mission of weight 7-kg was launched by Indian rocket PSLV-C20 on 25 February 2013 at 800-km high polar orbits. The mission design consists of six nanosats (hence Constellation): two from Austria, two from Canada, and two from Poland. Each 7 kg nanosat carries an optical telescope of aperture 3-cm feeding an uncooled CCD. One instrument in each pair is equipped with a blue filter; the other with a red filter. Each BRITE instrument has a wide field of view ( $\approx 24$  degrees), so up to about 15 bright stars can be observed simultaneously, sampled in 32 pixels x 32 pixels sub-rasters (Kuschnig & Weiss 2009).

Looking even farther to the future an European Space Agency “Cosmic Vision 2015–2025” proposal called PLANetary Transits and Oscillations of stars (PLATO) has been selected for ESAs M3 expected to launch in 2022–2024 to providing accurate key planet parameters (radius, mass, density and age) in statistical numbers it addresses fundamental questions such as: How do planetary systems form and evolve? The PLATO 2.0 instrument consists of 34 small aperture telescopes (32 with 25-sec readout cadence and 2 with 2.5- sec cadence) providing a wide field-of-view ( $22 \times 32 \text{ deg}^2$ ) and a large photometric magnitude range (4–16 mag). Asteroseismology will be performed for these bright stars to obtain highly accurate stellar parameters, including masses and ages (Rauer 2013).

## 15. 3.6-m Optical Telescope at Devasthal

The photon and scintillation are two dominating source of noise that play important role in the detection of the low-amplitude pulsational variability. Both of these noise can be minimized by observing with a bigger telescopes located at a good observing site. To reduce the scintillation noise for the detection of the low-amplitude light variations, a 3.6-m telescope at Devasthal site (longitude:  $79^\circ 40' 57''$  E, latitude :  $29^\circ 22' 26''$  N, altitude : 2420-m) has been installed and the first light is expected to be seen by mid of year 2015. Fig. 25 shows a picture of fully assembled 3.6-m telescope at Devasthal. In



Figure 25 : A picture of fully assembled 3.6-m telescope at Devasthal site.

the following subsections, we discuss the back-end instruments to be developed at ARIES for the asteroseismic study of pulsating variables.

### 15.1 *Time-Series Photometers*

For the asteroseismic study of the transient phenomena we are developing a single-channel (focal reducer) and three-channel high-speed time-series CCD photometer for the 3.6-m telescope. The scientific objective behind the building of these instruments is to perform asteroseismic study of transient events such as CP stars, white dwarfs, cataclysmic variables, red giants, open star clusters, detection of the extra-solar planetary systems.

## 15.2 *Optical Design of the Time-series Photometers*

The starting point of optical design of an instrument is to decide the required field of view (FoV) which should be large enough to have two- to three-comparison stars of comparable brightness and color to the target star. The probability of finding a comparison star of a given magnitude depends upon the search radius and the galactic latitude of the star (Simons et al. 1995). For example the probability of finding a comparison star for a 12 mag star at galactic latitude of  $30^\circ$  is 80 per cent if the search radius of 5 arcmin. Most of the target sources to be observed from 3.6-m telescope are expected fainter than 12 magnitude so a field of view of 6 arcmin virtually guarantees the presence of a suitable comparison stars.

### 15.2.1 *Single-Channel Photometer*

Fig. 26 shows the preliminary optical design of a single-channel photometer for the side port of 3.6-m telescope. A total of ten optical elements are used to reduce the focal length to produce required FoV. The design was driven using an exit-pupil far behind the last collimator lens. This locates the pupil close or inside the cameras, simplifying the camera design and reducing the size of camera lenses. The collimator has not been designed to avoid ghost-image issues that would result from a non-parallel beam passing through the thick filters/dichroics. Optimization was done on the complete telescope–collimator–camera combination without varying any parameters of the telescope. This allowed us to benefit from additional degrees of freedom without having the image quality of the collimator. Collimator contains four lenses and camera contains five lenses. The last lens is a field flattener that corrects the combined field curvature from telescope, collimator and camera. The field lens also acts as the vacuum seal of the cryostat. This avoids the need for an additional plane vacuum window and thus reduces Fresnel reflections. The collimator and camera are optimized combinedly with filter and detector window.

### 15.2.2 *Three-Channel Focal Reducer*

A single-channel photometer can be used to observe stars in a single band. For multi-band photometric observations this gives poor time-resolution. Hence we decided to develop a three-channel fast CCD photometer for observations of pulsating variables in three colors simultaneously. The optical design of the three-channel photometer is modified from the single-channel photometer by inserting fused silica dichroic beam splitters and N-BK7 SDSS filters. Fig. 27 shows the preliminary optical design of the three-channel photometer made for the axial port of 3.6-m telescope. The design consists of a four element collimator and three same set of five camera lenses collecting



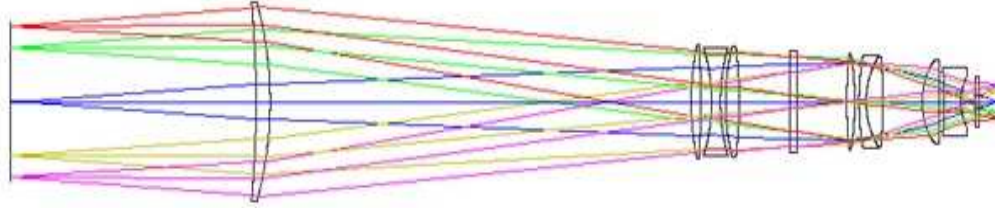


Figure 26 : The optical design of the single-channel CCD photometer.

the beam from dichroic beam splitters and send it to the detector through filters.

### 15.3 Detectors

The choice of detector for these instruments is frame transfer based CCD. To have the high-quantum efficiency (more than 80%) in the wavelength range  $4500 \text{ \AA} - 7500 \text{ \AA}$ , we prefer thin and back illuminated CCD. In the market the maximum no. of pixels in such CCDs are  $1024 \times 1024$  each of size  $13 \mu$  a side. The chip will be cooled by a three-stage thermo-electric cooler (TEC) based on the Peltier effect.

### 15.4 Filters

For the high-speed time-series photometry we plan to use both the standard SDSS  $u, g, r, i, z$  and Johnson Cousins  $U, B, V, R_c, I_c$  filters. Provision for the broad band filter BG40 made of Scott glass would be useful for the asteroseismic observations of pulsating white dwarfs.

### 15.5 System Throughput

The performance of an instrument depends upon the optimization of its throughput. Therefore to observe the objects of a wide range of brightness one would like to know the Signal-to-Noise (S/N) ratio achievable for a given set of exposure times. Given the transmission coefficients of the mirrors, filters, CCD glass, brightness of sky, extinction, quantum efficiency of the CCD chip, the S/N ratio can be calculated using the formula given by Mayya et al. (1991). If the sky brightness and the CCD input parameters like pixel size, dark current, read out noise are known then one can calculate the sky counts, the underlying S/N ratio and photometric accuracy (McLean 1989).

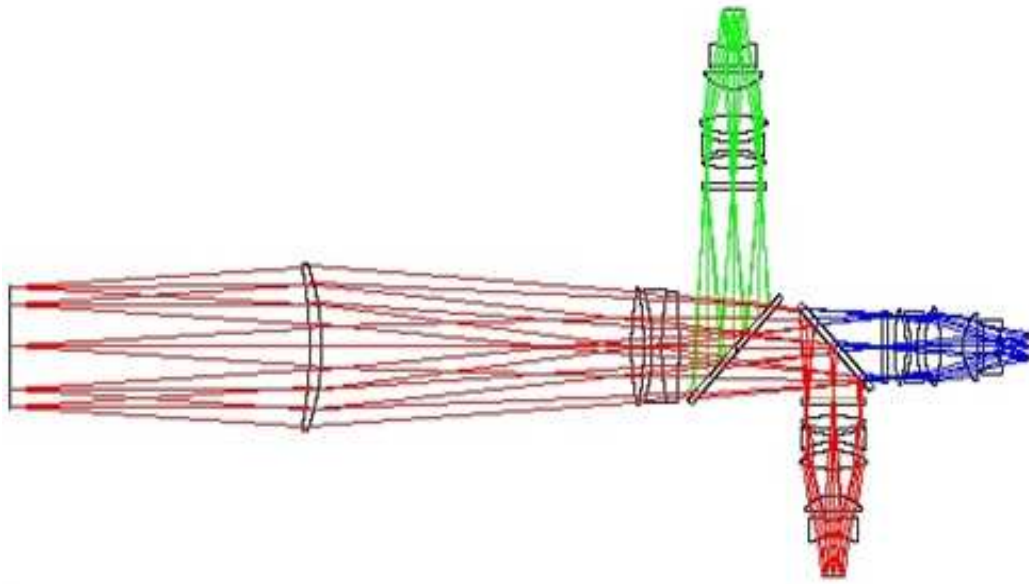


Figure 27 : The optical design of the proposed three-channel CCD photometer.

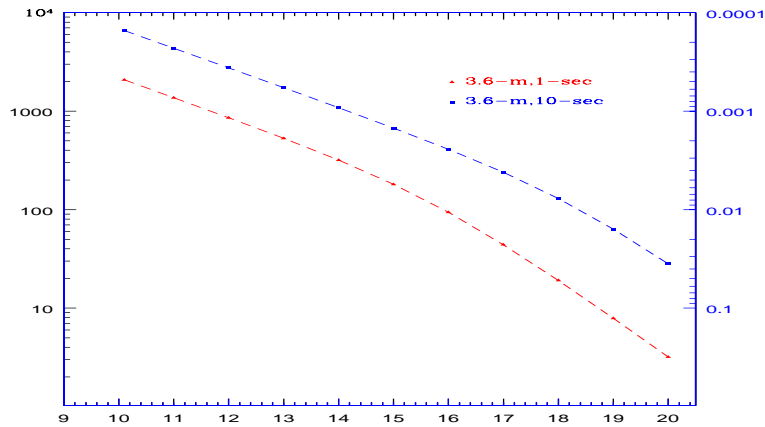


Figure 28 : A plot of B-band magnitude versus the calculated signal-to-noise ratio (y-axis, left) and corresponding error in the magnitude determinations (y-axis, right) for exposure times 1-sec and 10-sec for single-channel time-series CCD photometer for the 3.6-m telescope.

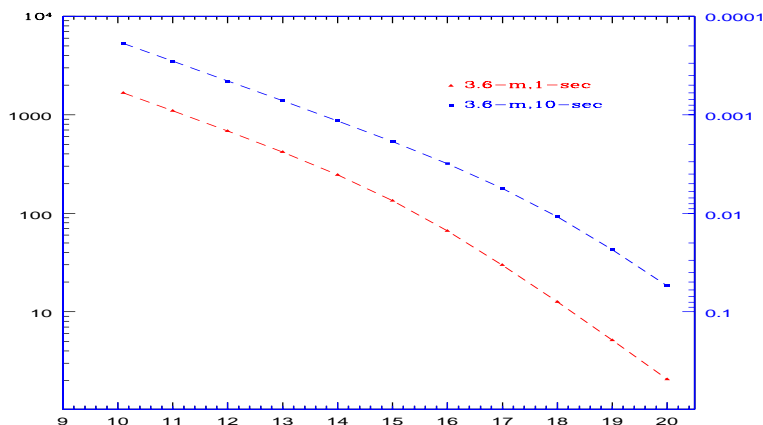


Figure 29 : Similar to Fig. 28 but for V-band.

We have calculated the system throughput for the single-channel photometer to be equipped at the side port of 3.6-m telescope. Fig. 28 and 29 show the B and V-band detection limit of the 3.6-m telescope for the stars of magnitude range 10 to 20 with exposure time 1 and 10-sec. From this figure it is evident that for the 3.6-m telescope the photometric precision of 0.01 mag in B-band can be achieved for stars of 17.5 mag and 18.5 mag with same exposure time. These figures also show the detection limit in the B and V-band, respectively with the same exposure time.

## 16. Conclusion

Asteroseismology is an unique approach for the investigation of stellar structure and evolution which has significantly improved our knowledge in last decades. Though asteroseismology is still in its infancy and far from the helioseismology however the high-precision ground and space based data will allow us to make the seismic analysis so robust that one can obtain the reliable information on the internal structure of stars. It is true that the space based time-series data are better than the ground-based in terms of accuracy and higher duty cycle but the ground based observations are more flexible in the selection of targets, time and duration of observations. The successful asteroseismology programme looks set to continue in the re-purposed Kepler Mission, K2 (Chaplin et al. 2013; Howell et al. 2014). Observationally, the longitude of India makes this region critical to all global observational helioseismic and asteroseismic studies to fill the gap in the time-series data. The presence of 4-m class optical telescope in the Asian region would be very useful for asteroseismic study of faint pulsating variables. At ARIES

we are developing a single and three-channel fast CCD photometers to optimized for the high-speed time-series measurements and looking forward for their commissioning. In the future, the asteroseismology of many thousands of stars in various stages of their evolution will enable us to tackle several long-standing problems, such as stellar dynamos, stellar convection.

## Acknowledgments

SJ dedicates this review article to his mother Late Smt. Ganga Joshi. SJ is grateful to the SOC of the Indo-UK seminar for the invitation to deliver an invited talk on the topic “Asteroseismology from ARIES”. We acknowledge Prof. Ram Sagar, Prof. D. W. Kurtz, Dr. Peter Martinez, Dr. S. Seetha and Dr. B. N. Ashoka for initiating the field of Asteroseismology at ARIES. The authors are thankful to the anonymous referee for providing the remarkable comments that improved the manuscript drastically. SJ acknowledge to Sowgata Chaudhary for reading the manuscript carefully and pointing out the typos. The optical design of the time-series photometer has been done by Er. Krishna Reddy. This is the compilation of work done under the Indo-Russian RFBR project INT/RFBR/P-118.

## References

- Aerts Conny, Christensen-Dalsgaard Jorgen, Kurtz Donald W., 2010, *Asteroseismology*, Astronomy and Astrophysics Library. ISBN 978-1-4020-5178-4. Springer Science, Business Media B.V., 2010
- Althaus L. G., Corsico A. H., Isern J. & Garcia-Berro, E. 2010, *A&AR*, 18, 471
- Antoci V., Handler G., Campante T. L. et al. 2011, *Nature*, 77, 570
- Appourchaux T., Belkacem K.; Broomhall A.-M. et al. 2010, *A&AR*, 18, 197
- Appourchaux T., Grundahl F. 2013, arXiv:1312.6993
- Ashoka B. N., Kumar Babu V. C., Seetha S., Girish V. et al. 2001, *JApA*, 22, 131
- Auvergne M., Bodin P., Boisnard L. et al. 2009, *A&A*, 506 411
- Baglin, A., Auvergne, M., Barge, P., Deleuil, M., Michel, E. and the CoRoT Exoplanet Science Team 2009, in *Proc. IAU Symp. 253, Transiting Planets*, eds F. Pont, D. Sasselov & M. Holman, IAU and Cambridge University Press, p. 71
- Balona L. A., Krisciunas K., Cousins A. W. J., 1994, *MNRAS*, 270, 905
- Balona L. A., 2010, *Challenges In Stellar Pulsation* by L.A. Balona. eISBN: 978-1-60805-185-4, Bentham Publishers
- Balona L. A., Pigulski A., De Cat P., Handler G., Gutierrez-Soto J. et al. 2011, *MNRAS*, 413, 2403
- Balona L. A., Joshi S., Joshi Y. C., Sagar R., 2013, *MNRAS*, 429, 1466
- Balona L. A., 2014, *MNRAS*, 439, 3453
- Barnes S. A., 2009, in *IAU Symposium, Vol. 258, IAU Symposium*, ed. E. E. Mamajek, D. R. Soderblom, & R. F. G. Wyse, 345
- Basu S. & Antia H. M., 2008, *Physics Reports*, 457, 217
- Bedding T. R., Zijlstra Albert A., Jones A., Foster G., 1998, *MNRAS*, 301, 1073

- Bedding T. R., & Kjeldsen H. 2003, *PASA*, 20, 203
- Bedin L. R., King I. R., Anderson J. et al. 2008, *ApJ*, 678, 1279
- Belkacem K., Samadi R., Goupil M.-J., Dupret M.-A. 2008, *A&A*, 478, 163
- Bigot L. & Dziembowski W. A., 2002, *A&A*, 391, 235
- Blazhko S., 1907, *AN*, 175, 325
- Breger M. & Bregman, J. N. 1975, *ApJ*, 200, 343
- Breger M., 1979, *PASP*, 91, 5
- Breger M., Stich J., Garrido R. et al. 1993, *A&A*, 271, 482
- Breger M., 2000, *Delta Scuti and Related Stars*, 210, 3
- Breger M., Lenz P., Antoci V., Guggenberger E., Shobbrook R. R. et al. 2005, *A&A*, 435, 955
- Briquet M., Morel T., Thoul A. et al. 2007, *MNRAS*, 381, 1482
- Brogaard K., Bruntt H., Grundahl F. et al. 2011, *A&A*, 525, 2
- Brown Timothy M. & Gilliland, Ronald L., 1994, *ARA&A*, 32 37
- Bruntt H., Kervella P., Merand A. et al. 2010, *A&A*, 512, 55
- Buzasi D. L., Catanzarite J., Conrow T. et al. 2000, *ApJ*, 532, L133 1
- Castanheira B.G., Kepler S.O., Kleinman S. J., Nitta A., & Fraga L., 2013, *MNRAS*, 430, 50
- Chanamé J. & Ramírez I., 2012, *ApJ*, 746, 102
- Chaplin W. J., Elsworth Y., Howe R., Isaak G. R. et al. 1996, *Sol. Phys.*, 168, 1
- Chaplin W. J., Serenelli, Aldo M. et al. 2007, *ApJ*, 670, 827
- Chaplin W. J. & Basu Sarbani, 2008, *Sol. Phys.*, 251, 53
- Chaplin W. J., Appourchaux T., Elsworth, Y., Garca R. A., Houdek G. et al. 2010, *ApJ*, 713L, 169
- Chaplin W. J., Kjeldsen H., Bedding T. R. et al. 2011a, *ApJ*, 732, 54
- Chaplin W. J., Kjeldsen H., Christensen-Dalsgaard J. et al. 2011b, *Science*, 332, 213
- Chaplin W. J. & Miglio, A., 2013, *ARAA*, 51, 353
- Chaplin W. J., Basu S., Huber, D., Serenelli A. et al. 2014, *ApJS*, 210, 1
- Christensen-Dalsgaard J. & Frandsen S., 1983, *Solar Phys.*, 82, 469
- Christensen-Dalsgaard, J. 1984, in *Space Research in Stellar Activity and Variability*, ed. A. Mangeney & F. Praderie, 11
- Christensen-Dalsgaard J & Berthomieu, Gabrielle, *Solar interior and atmosphere (A92-36201 14-92)*, 1991, Tucson, AZ, University of Arizona Press, p. 401-478. Research supported by SNFO and CNRS.
- Christensen-Dalsgaard J., Bedding T. R. & Kjeldsen H., 1995, *ApJ*, 443, L29
- Christensen-Dalsgaard J. & Dziembowski, W. A. 2000, in *Variable Stars as Essential Astrophysical Tools*, eds. C. Ibanoglu, Kluwer Acad. Publ., Dordrecht, 544, 1
- Christensen-Dalsgaard J., 2002, *Reviews of Modern Physics*, vol. 74, Issue 4, 1073
- Corsico A. H., Althaus, L.G., Montgomery, M. H., García-Berro, E., & Isern, J. 2005, *A&A*, 429, 277
- Cox J. P. & Whitney C., 1958, *ApJ*, 127, 561
- Cox J. P., 1980, *Theory of stellar pulsation*, Research supported by the National Science Foundation Princeton, NJ, Princeton University Press, 1980.
- Daszyńska-Daszkiewicz, J., Dziembowski, W. A., Pamyatnykh, A. A. 2005, *A&A*, 441, 641
- De Cat P., Eyser L., Cuyppers J. et al. 2006, *A&A*, 449, 281

- De Ridder J., Telting J. H., Balona L. A. et al. 2004, MNRAS, 351, 324  
De Ridder J., Barban C., Baudin F. et al. 2009, Nature, 459, 398  
Deubner F.-L., 1975, Solar Phys., 40, 333  
Di Mauro, M. P.; Christensen-Dalsgaard, J.; Kjeldsen, H.; Bedding, T. R.; Patern, L., 2003a, A&A, 404, 341  
Di Mauro, Maria Pia; Christensen-Dalsgaard, J.; Paterno, Lucio, 2003b, Ap&SS, 284, 229  
Di Mauro M. P. et al. 2004, Solar Phys., 220, 2, 185  
Di Mauro M. P. 2013, Mem. S.A.It., 84, 325  
Dravins D., Lindegre, L., Mezey E., Young A. T., 1998, PASP, 110, 610  
Dziembowski W. A., 1977, AcA, 27, 203  
Dziembowski W. A. & Cassisi S., 1999, AcA, 49, 371  
Dziembowski W. A. & Goode P. R., 1996, ApJ, 458, 338  
Dziembowski W. A., Goode P. R., Schou J., 2001, ApJ, 553, 897  
Dupret M.-A., De Ridder J., De Cat et al. 2003, A&A, 398, 677  
Eggenberger P., Udry S., Mayor M., A&A, 2004, 417, 235  
Elkin V. G., Kurtz D. W., Mathys G., 2005, MNRAS, 364, 864  
Fletcher Stephen T., Broomhall, Anne-Marie, Salabert, David et al., 2010, ApJ, 718L, 19  
Gao X.-H., & Chen L. 2012, Chinese Astronomy and Astrophysics, 36, 1 1  
Garcí R. A., Jiménez A., Mathur S., Ballot J. et al. 2008, AN, 329, 476  
García, R. A., Ceillier, T., Mathur, S., Salabert, D. 2013, ASPC, 479, 129  
Garg A., Cook K. H., Nikolaev S., Huber M. E., Rest A., 2010, AJ, 140, 328  
Garnavich P. M., Vandenberg D. A., Zurek D. R., Hesser, J. E., 1994, AJ, 107, 1097  
Garrido R., Garcia-Lobo E., & Rodriguez E., 1990, A&A, 234, 262  
Gautschy A., & Saio H., 1993, MNRAS, 262, 213  
Gilliland R. L., Brown T. M., Kjeldsen H. et al. 1993, AJ, 106, 2441  
Girish V., Seetha S., Martinez P., Joshi S. et al. 2001, A&A, 380, 142  
Goldreich, P., & Keeley D. A., 1977, ApJ, 212, 243  
Goldreich P., Murray N., Kumar, P., 1994, ApJ, 424, 466  
Goupil M. J. 2009, in Lecture Notes in Physics, Berlin Springer Verlag, Vol. 765, The Rotation of Sun and Stars, ed. J.-P. Rozelot & C. Neiner, 45  
Goupil Marie-jo, 2011, arXiv1102, 1884  
Grec G., Fossat E., Pomerantz M. A., 1983, Solar Physics, 82, 55  
Grigahcène A., Antoci V., Balona L., Catanzaro G. et al. 2010, ApJ, 713L, 192  
Grundahl, F., Christensen-Dalsgaard, J., Arentoft, T., Frandsen, S. et al. 2009, CoAst, 158, 345  
Grundahl, F., Christensen-Dalsgaard, J., Grae Jrgensen, U., et al. 2011, Journal of Physics Conference Series, 271, 012083  
Guenther D. B. & Demarque P., 2000, ApJ, 531, 503  
Guenther D. B., 2004, ApJ, 612, 454  
Guzik Joyce A., Kaye, Anthony B. et al. 2000, ApJ, 542L, 57  
Handler G., Balona L. A., Shobbrook R. R. et al. 2002, MNRAS, 333, 262  
Handler G. & Shobbrook R. R., 2002, ASPC, 256, 117  
Handler G., Shobbrook R. R., Vuthela F. F. et al. 2003, MNRAS, 341, 1005  
Handler G., Jerzykiewicz M., Rodriguez E. et al. 2006, MNRAS, 365, 327  
Hareter M., Reegen P., Kuschnig R., 2008, CoAst, 156, 48  
Harvey J. W., Hill F., Hubbard R. et al. 1996, Science 272, 1284

- Hatzes A. P. & Mkrtychian D. E., 2004, *MNRAS*, 351, 663
- Heber U., 2009, *ARAA*, 47, 211
- Hekker S., Basu, S., Stello, D., et al. 2011, *A&A*, 530, 100
- Hekker S., Elsworth Y., Basu S. et al. 2013, *MNRAS*, 434, 1668
- Henry Gregory W., Fekel Francis C., Henry Stephen M., 2005, *AJ*, 129, 2815
- Hole K. T., Geller A. M., Mathieu R. D. et al. 2009, *AJ*, 138, 159
- Houdek G., Balmforth N. J., Christensen-Dalsgaard J., Gough D. O., 1999, *A&A*, 351, 582
- Howell S. B., Sobeck C., Haas M., et al. 2014, *PASP*, 126, 398
- Huber D., Bedding, T. R., Stello, D. et al. 2010, *ApJ*, 723, 1607
- Huber D., Bedding T. R., Stello D. et al. 2011, *ApJ*, 743, 143
- Jeffery C. S., Ramsay G., 2014, *MNRAS*, 442, L61
- Jeffery C. S., Dhillon V. S., Marsh T. R., Ramachandran B., 2004, *MNRAS*, 352, 699
- Joshi S., Girish, V., Sagar R., Kurtz D. W. et al. 2003, *MNRAS*, 344, 431
- Joshi S., Mary D. L., Martinez P., Kurtz, D. W. et al. 2006, *A&A*, 455, 303
- Joshi S., Mary D. L., Chakradhari N. K., Tiwari, S. K., Billaud, C., 2009, *A&A*, 507, 1763
- Joshi Y. C., Joshi S., Kumar B., Mondal S., Balona L. A., 2012a, *MNRAS*, 419, 2379
- Joshi S., Semenko E., Martinez P. Sachkov M., Joshi Y. C. et al. 2012b, *MNRAS*, 424, 2002
- Kallinger, T., Mosser, B., Hekker, S. et al. 2010, *A&A*, 522, 1
- Kanaan A., Nitta A., Winget D.E. et al. 2005, *A&A*, 432, 219
- Kawaler Steven D., Sekii T., Gough D., 1999, *ApJ*, 516, 349
- Kepler S. O., Costa J. E. S., Castanheira B. G., Winget D. E., Mullally Fergal et al. 2005, *ApJ*, 634, 1311
- Khomenko E. & Kochukhov O., 2009, *ApJ*, 704, 1218
- Kilkenny, D., Koen, C., O'Donoghue, D. & Stobie, R. S., 1997, *MNRAS*, 285, 640
- Kilkenny D., Reed M. D., ODonoghue D., Kawaler S. D., Mukadam A., Kleinman S. J., Nitta A., 2003, *MNRAS*, 345, 834
- Kjeldsen H. & Bedding T. R., 1995, *A&A*, 293, 87
- Kjeldsen, H., Bedding, T. R., Viskum, M. & Frandsen, S. 1995, *AJ*, 109, 1313
- Koch D. G., Borucki W. J., Basri G. et al. 2010, *ApJ*, 713, L79
- Kochukhov O., 2004, *A&A*, 423, 613
- Kochukhov O., Bagnulo S., Lo Curto, G., Ryabchikova T., 2009, *A&A*, 493L, 45
- Kolenberg K. 2008, in Proc. HELAS II International Conference: Helioseismology, Asteroseismology and the MHD Connections, eds L. Gizon & M. Roth, J. Phys.: Conf. Ser., 118, 012060
- Kolenberg K. et al. 2010, *ApJ*, 713, 198
- Kumar P. & Goldreich P. 1989, *ApJ*, 342, 558
- Kurtz D. W., 1982, *MNRAS*, 200, 807
- Kurtz D. W., Matthews J. M., Martinez P., Seeman J.m Cropper, M. et al. 1989, *MNRAS*, 240, 881
- Kurtz D. W., Kawaler S. D., Riddle R. L., Reed M. D., Cunha M. S., Wood M., Silvestri N., 2002, *MNRAS*, 330, L57
- Kurtz D. W., Cameron C., Cunha M. S. et al. 2005, *MNRAS*, 358, 651
- Kurtz D. W., 2006, *ASP*, Volume 349, 101, *Astrophysics of Variable Stars*, eds C.

- Sterken & C. Aerts
- Kurtz D. W., Cunha, M. S., Saito H. et al. 2011, MNRAS, 414, 2550
- Kuschnig, R. & Weiss, W. W., 2009, CoAst, 158, 351
- Leavitt H. S. & Pickering, Edward C., 1912, Harvard College Observatory Circular, vol. 173, pp.1-3
- Ledoux P., 1951, ApJ, 114, 373
- Leibacher J. W., Stein, R. F., 1971, ApL, 7, 191L
- Leighton R. B., Noyes R. W., Simon G. W., 1962, ApJ, 135 47
- Lignières F. & Georgeot B. 2009, A&A, 500, 1173
- Majaess D., Turner D., Gieren W., 2011, ApJ, 741L, 36
- Mantegazza L., Poretti E., Michel E., Rainer M., Baudin F., García Hernández A., 2012, A&A, 542, 24
- Martinez P., Kurtz D. W., Ashoka B. N. et al. 2001, A&A, 371, 1048
- Mayya Y. D. 1991, JApA, 12, 319
- McLean I. S., 1989, in *Electronic and Computer -Aided Astronomy*, Ellis Horwood, Chichester
- Metcalf T. S., Montgomery M. H., & Kanaan A., 2004, ApJ, 605, L133
- Metcalf T. S., Creevey O. L., Christensen-Dalsgaard J., 2009, ApJ, 699, 373
- Miglio A., Brogaard, K., Stello, D. et al. 2012, MNRAS, 419, 2077
- Michel, E., Baglin A., Weiss W. W., Auvergne M., Catala C. et al. 2008, Comm. in Asteroseismology, 156, 73
- Montgomery M. H., & Winget D. E. 1999, ApJ, 526, 976
- Morel P., Provost J., Lebreton Y. et al. 2000, A&A Vol. 363, 675
- Moskalik, P., 1995, ASPC, 83, 44
- Mosser B. & Aristidi E., 2007, PASP, 119, 127
- Mukadam Anjum S., Kepler S. O., Winget D. E., Nather, R. E., Kilic M. et al. 2003, ApJ, 594, 961
- Olbers W. 1850, *Astronomische Nachrichten*, 31, 129
- Ostensen R. H., Pápics P. I., Oreiro R., Reed M. D. et al. 2011, ApJ, 731L, 130
- Ouazzani R.-M. & Goupil M.-J. 2012, A&A, 542, A99
- Pamyatnykh A. A., 1999, AcA, 49, 119
- Pamyatnykh A. A., 2003, PASP 284, 97
- Pepe, F., Mayor, M., Delabre, B., et al. 2000, in *Society of Photo-Optical Instrumentation Engineers (SPIE) Conference Series*, Vol. 4008, Society of Photo-Optical Instrumentation Engineers (SPIE) Conference Series, ed. M. Iye & A. F. Moorwood, 582592
- Perryman M. A. C. & ESA 1997, ESA Special Publication, 1200 1
- Petersen J. O. & Christensen-Dalsgaard J., 1999, A&A, 352, 547
- Pigott E. 1785, *Royal Society of London Philosophical Transactions Series I*, 75, 127
- Pych W., Kaluzny J., Krzeminski W., Schwarzenberg-Czerny A., Thompson I. B., 2001, A&A, 367, 148
- Rauer H., Catala C., Aerts C., Appourchaux T. et al. 2013, arXiv1310.0696
- Reese D. R. 2010, *Astronomische Nachrichten*, 331, 1038
- Rhodes E. J. Jr., Ulrich R. K., Simon G. W., 1977, ApJ, 218, 901
- Ryabchikova T., Sachkov M., Weiss W. et al., A&A, 2007, 462, 1103
- Sachkov M., Kochukov O., Ryabchikova T. et al. 2008, MNRAS, 389, 903
- Sachkov, M. Hareter M., Ryabchikova T. et al., 2011, MNRAS, 416, 2669



- Saio H. & Gautschy A., 1998, *ApJ*, 498, 360
- Salabert D., Leibacher J., Appourchaux T., Hill F., 2009, *ApJ*, 696, 65
- Samadi R., & Goupil M.-J., 2001, *A&A*, 370, 136
- Samadi R., Nordlund A., Stein R. F., Goupil M. J., Roxburgh I., 2003, *A&A*, 403, 303
- Samadi R., Belkacem K., Goupil M.-J., Ludwig H.-G., Dupret M.-A., 2008, *Communications in Asteroseismology*, 157, 130
- Shapley H., 1914, *ApJ*, 40, 448
- Simons Douglas A., Robertson David J., Mountai C. Matt, 1995, *SPIE*, 2475, 296
- Soszynski I., Poleski R., Udalski A. et al. 2010, *Acta Astronomica*, 60, 17
- Stankov A., Handler G., 2005, *ApJS*, 158, 193S
- Stellingwerf R. F., 1979, *ApJ*, 227, 935
- Stello D., Bruntt H., Arentoft T., Gilliland R. L. et al. 2007a, *CoAst*, 150, 149
- Stello D.; Bruntt H.; Kjeldsen H.; Bedding T. R., Arentoft T. et al. 2007b, *MNRAS*, 377, 584
- Stello D., Bruntt H., Preston H., Buzasi D. 2008, *ApJ*, 674, L53
- Stello Dennis & Gilliland, Ronald L., 2009, *ApJ*, 700, 949
- Stello D., Basu S., Brunt, H. et al. 2010, *ApJ*, 713, L182
- Stell, D., Huber D., Kallinger T. et al. 2011a, *ApJ*, 737, L10
- Stello D., Meibom S., Gilliland R. L. et al. 2011b, *ApJ*, 739, 13
- Stetson P. B., 1987, “DAOPHOT - A computer program for crowded-field stellar photometry”, *Publications of the Astronomical Society of the Pacific*, 99, 191–222
- Suárez J. C., Garrido R., Moya A., 2007, *AA* 474, 971
- Suárez J. C., Goupil M. J., Reese D. R. et al. 2010, *ApJ*, 721, 537
- Szabó R., Kollath Z., Molnar L., Kolenberg K., Kurtz D. W. et al. 2010, *MNRAS*, 409, 1244
- Tabur V., Beddin, T. R. Kiss L. et al. 2009, *MNRAS*, 400, 194
- Takata Masao & Shibahashi Hiromoto, 1995, *PASJ*, 47, 219
- Takata M., 2012, *PASJ*, 64, 66
- Tassoul M. 1980, *ApJS*, 43, 469 2
- Telting J. H., & Schrijvers, C., 1997, *A&A* 317, 723
- Telting J. H., 2003, *Ap&SS*, 284, 85
- Templeton M., Basu, S., Demarque, P., 2002, *ApJ*, 576, 963
- Thévenin F., Provost, J., Morel P. et al. 2002, *A&A*, 392, L9
- Ulrich Roger K., 1970, *ApJ*, 162, 993
- Ulrich R. K., 1986, *ApJ*, 306, L37
- Unno W., Osaki Y., Ando H., Saio H., Shibahashi H., 1989, *Nonradial oscillations of stars*, 2nd edition, Tokyo: University of Tokyo Press
- Uytterhoeven K., Mathias P., Poretti E. et al. 2008, *A&A*, 489, 1213
- Vauclair G., Moskalik P., Pfeiffer B. et al. 2002, *A&A*, 381, 122
- Vauclair G., Vauclair S., Pamjatnikh A., 1974, *A&A*, 31, 63
- Walker G., Matthews Jaymie, Kuschnig Rainer et al. 2003, *PASP*, 115, 1023
- White T. R., Bedding T. R., Stell D. et al. 2011, *ApJ*, 743, 161
- White Timothy R., Bedding Timothy R., Gruberbauer Michael, Benomar Othman et al. 2012, *ApJ*, 751L, 36
- Winget D. E., van Horn H. M., Tassoul M., Fontaine G., Hansen C. J., Carroll, B. W. 1982, *ApJ*, 252, L65

- Winget D. E. & Kepler S. O., 2008, ARAA, 46, 157  
Wood P. R., 1995, ASPC, 83, 127  
Woodard M. & Hudson H., 1983, Sol. Phys., 82, 67  
Wu T. Li Y. & Hekker S., 2014a, ApJ, 781, 44  
Wu T. Li Y. & Hekker S. 2014b, ApJ, 786, 10  
Zima W., Wright D., Bentley J. et al. 2006, A&A, 455, 235  
Zhevakin S. A., 1963, ARA&A, 1, 367